Environmental Impact Assessment Review 98 (2023) 106942

Contents lists available at ScienceDirect

Environmental Impact Assessment Review

journal homepage: www.elsevier.com/locate/eiar

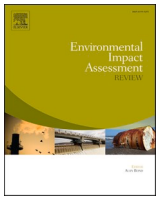

Energy potentials, negative emissions, and spatially explicit environmental impacts of perennial grasses on abandoned cropland in Europe

Cristina-Maria Iordan *, Baptiste Giroux, Jan Sandstad Næss, Xiangping Hu, Otávio Cavalett, Francesco Cherubini

Industrial Ecology Program, Department of Energy and Process Engineering, Norwegian University of Science and Technology, N-7491 Trondheim, Norway

ARTICLE INFO

Keywords:
Bioenergy
Negative emissions
LCA
SOC
Perennial grasses
Abandoned cropland

ABSTRACT

Cultivating perennial grasses on abandoned cropland for bioenergy production is a promising option to meet future renewable energy demands at lower risks for food security and environmental degradation. Studies on the potential environmental impacts of perennial grasses mostly focus on specific locations, while effects and potentials of a large-scale deployment on abandoned cropland are still unexplored. This work performs a spatially explicit life cycle assessment of agricultural production of three perennial grasses (miscanthus, switchgrass, and reed canary grass) on abandoned cropland in Europe under rainfed and irrigated conditions. We estimate the primary bioenergy potentials and potential environmental impacts on climate change (including soil organic carbon changes), freshwater and marine eutrophication, terrestrial acidification, fossil resource scarcity and water scarcity footprint. Under rainfed conditions, switchgrass has the largest supply potential (174 Mt_{DM} yr^{-1}) while miscanthus has the lowest average climate impact (169 kg CO_2 t_{DM}^{-1}). Irrigation increases biomass yields by 97% for miscanthus, 62% for switchgrass and 29% for reed canary grass, but climate change impacts per t_{DM} increase by 24%, 32% and 44%. Water scarcity footprints also increase, ranging from 4.7 to 9 world m^3eq. kg_{DM}^{-1}. When soil organic carbon changes are considered, the net climate effects turn to negative for all perennial grasses under rainfed conditions (and for miscanthus with irrigation as well), showing a potential for land-based negative emissions by storing carbon in soils while delivering renewable energy. Bioenergy potentials range between 1 and 7 $EJyr^{-1}$ (corresponding to 1–10% of today's EU primary energy demand) and the scale of negative emissions can be up to −24 Mt. CO_2-eq. yr^{-1} (equal to 5.6% of EU's agricultural sector emissions). The consideration of site-specific conditions for water supply and crop affinity can identify the best local agricultural practices for energy yields and negative emissions at reduced environmental trade-offs.

1. Introduction

Climate change mitigation scenarios aiming to achieve the most stringent temperature targets rely on substantial amounts of bioenergy from dedicated crops (Shukla et al., 2019). In the 1.5 °C pathways, the bioenergy share in the global primary energy supply is estimated to grow from today's 10% to 23–27% in 2050 (Rogelj et al., 2018). In the Shared Socio-economic Pathways (SSP) compatible with the lowest levels of climate change, bioenergy feedstock supply ranges from 5300 to 23,000 Mt. of dry matter (DM) per year by the end of the century (Popp et al., 2017). This corresponds to an estimated 245 to 1517 Mha of land for dedicated bioenergy crops. Bioenergy crops are expected to play such a key role because they provide opportunities to cut emissions in the energy and transport sectors while allowing for atmospheric carbon removal when coupled with carbon capture and storage (CCS) technologies (Bauer et al., 2018; Hanssen et al., 2019; Daioglou et al., 2019).

However, concerns have been raised regarding potential sustainability trade-offs of a large-scale deployment of bioenergy crops (Humpenöder et al., 2018; Smith et al., 2019). Besides supplying renewable energy for climate change mitigation, land use is part of a nexus with other key global environmental challenges, such as feeding the increasing global population, protecting natural ecosystems, and maintaining water resources (Popp et al., 2017; Smith et al., 2020; McElwee et al., 2020). Increased competition with other land uses may be a threat to food security and natural ecosystems (Smith et al., 2013), and the net environmental benefits of bioenergy crops may vary with the type of crop, agricultural management intensity, and previous land use (Creutzig et al., 2015; Field et al., 2020). Successful strategies for

* Corresponding author.
E-mail address: cristina.m.iordan@ntnu.no (C.-M. Iordan).

https://doi.org/10.1016/j.eiar.2022.106942
Received 9 December 2021; Received in revised form 22 September 2022; Accepted 24 September 2022
Available online 10 October 2022

deployment of bioenergy crops need to rely on improvements in the agri-food sector (e.g., sustainable intensification, dietary changes, minimization of food waste, etc.) to spare land and decrease overall competition for land resources (Slade et al., 2014; Boysen et al., 2017). For example, by matching the more appropriate food crops with land availability and suitability across the globe, the land requirements for producing today's amount of food can be reduced by 50%, thereby showing the large land sparing potential for climate change mitigation objectives or nature restoration (Folberth et al., 2020).

Perennial grasses are usually drought-resistant crops, they can be grown at lower input requirements than annual crops and they help to improve soil quality and restore land degradation processes (Schmidt et al., 2015; Scordia and Cosentino, 2019; Robertson et al., 2017b). Due to their perennial nature, tillage and maintenance operation needs are lower when compared with annual crops (Heaton, 2004; Lewandowski, 2016). In addition, they may have positive environmental effects on restoring degraded land through reduced soil erosion and improved soil quality (Liu et al., 2012; Englund et al., 2020), as well as increasing biodiversity by providing habitat for birds and insects (Robertson et al., 2017b). Reduced soil disturbance from limited tillage, along with their deep root system, allows for high water use efficiency, recycling of nutrients and increases soil organic carbon (SOC), which further mitigates climate change (Zhu et al., 2018; Jones et al., 2016; Don et al., 2012). The transition from cropland to perennial grasses may also have a cooling effect on the regional climate as a result of biophysical effects such as increased evapotranspiration and albedo (Harding et al., 2016; Georgescu et al., 2011; Miller et al., 2016).

Life cycle assessment (LCA) is a key method for assessing environmental performance of products by accounting for the potential environmental impacts that arise over their full life cycle, including raw material acquisition, production, use and disposal (Cherubini et al., 2009; Pereira et al., 2019). Several studies have explored the life cycle performance of miscanthus (McCalmont et al., 2017; Fusi et al., 2020; Perić et al., 2018), switchgrass (Bai et al., 2010; Howard Skinner et al., 2012; Cherubini and Jungmeier, 2010) and reed canary grass (Shurpali et al., 2010), or combinations of them (Kiesel et al., 2016; Smeets et al., 2009; Bullard and Metcafe, 2001). They generally find from medium to large climate change mitigation benefits, but relatively high impacts for freshwater eutrophication and acidification, mostly driven by fertilization. Most of the studies are specific to a given location only, and studies specifically addressing the environmental performances on marginal or abandoned land are limited (Amaducci et al., 2017; Fernando et al., 2018; Schmidt et al., 2015).

Growing perennial grasses for bioenergy production on abandoned cropland has emerged as a sustainable approach to gradually expand bioenergy supply at reduced risks for land competition, food security and the environment (Robertson et al., 2017b; Muri, 2018; Daioglou et al., 2019). Agricultural abandonment is widespread in many regions of the world, including Europe (Ustaoglu and Collier, 2018; Levers et al., 2018), and it is driven by a combination of many socio-economic, political and environmental factors that undermine the profitability of formerly cultivated fields (Lasanta et al., 2017; Li and Li, 2017; Jepsen et al., 2015). Several studies have estimated the potentials and sustainability aspects of expanding bioenergy crops into abandoned cropland or marginal land, using a mix of different datasets to estimate land availability, crop yields, and geographical coverage (Leirpoll et al., 2021; Cintas et al., 2021; Albanito et al., 2016). For example, using marginal and degraded agricultural land for biofuel production can meet up to 55% of the current world liquid fuel consumption without using land under regular productivity for conventional crops or pasture (Cai et al., 2011). In Europe, an expansion of perennial biomass plantations on cropland areas prone to degradation or pollution can improve several sustainability indicators (Englund et al., 2020), and a strategic deployment targeting riparian buffers and wind breaks can co-deliver biomass production (up to 450 PJ) and improve land quality (Englund et al., 2021). Targeted incentives can stimulate the production of bioenergy crops on those lands with potential environmental, economic and social benefits (Rahman et al., 2019; Soldatos, 2015). No previous studies have specifically focused on the potentials and environmental impact implications of growing perennial grasses on abandoned cropland in Europe.

In this work, a bottom-up spatially explicit LCA is used to estimate the primary energy potentials and associated potential environmental impacts (at farm gate) of an idealized large-scale deployment of perennial grasses on abandoned cropland in Europe. The system boundaries include all processes required for biomass planting, cultivation, harvesting and transport up to farm gate (see Fig. S1 in Supplementary Information). The analysis integrates a gridded agro-ecological crop yield model (Global Agro-Ecological Zone 3.0 (GAEZ)) (Fischer et al., 2012) and a recently available map of abandoned cropland in Europe between 1992 and 2015 (Næss et al., 2021) to estimate yields of three perennial grasses (miscanthus, reed canary grass, switchgrass) and the grid-specific potential environmental impacts of their cultivation under two water supply conditions (rainfed and irrigated). The impact categories considered are climate change, terrestrial acidification, marine and freshwater eutrophication, fossil resource depletion and water scarcity footprint. The climate change results include a sensitivity to different climate metrics. The contributions of the changes in SOC from the establishment of perennial grasses on former cropland are estimated using a locally parameterized regression model (Ledo et al., 2020). Water scarcity footprints are computed using country specific characterization factors (Boulay et al., 2018), which highlight the areas where water resources can become a constraint in the long-term. Bioenergy potentials, co-benefits and trade-offs across multiple environmental impact indicators are explored both at a fine scale (300 m) resolution and aggregated at European level.

2. Methodology

2.1. Abandoned cropland and bioenergy yields

The identification of abandoned cropland in Europe relies on a recently produced dataset based on land cover maps from the European Space Agency Climate Change Initiative (ESA CCI) for the time period 1992–2015 (ESA, 2017; Næss et al., 2021). The ESA CCI-LC dataset integrates multiple satellite products and ground-truth observations to provide annual global maps of the earth's terrestrial surface at 300 m spatial resolution using 37 land classes based on the United Nation Land Cover Classification System (UNLCCS). Abandoned cropland was identified by monitoring all grids that were cropland in 1992 but not in 2015, so that all transitions from each of the six UNLCCS cropland classes to any other classes are considered, except the transitions to urban settlements (Næss et al., 2021).

Abandoned croplands in Europe are about 16 Mha (4% of cropland extent in Europe in 2015 (Santoro et al., 2017)) and are located across the entire continent, with major clusters in central and eastern Europe (Fig. 1). Several studies analyzed the main drivers and causes of cropland abandonment in Europe (Lasanta et al., 2017; Li and Li, 2017). They usually find that the abandonment process is mostly due to socioeconomic factors, such as economic growth, exposure to international markets (especially from countries linked to the former Soviet Union) and migration to urban areas, rather than declines in soil quality and fertility.

Three key perennial grasses that are adaptive to a large variety of climatic zones are considered in this work as bioenergy crops: miscanthus (*Miscanthus spp*), switchgrass (*Panicum virgatum*) and reed canary grass (*Phalaris arundinacea*). All three perennial grasses adapt to a wide variety of climate and soil conditions, and they can easily be incorporated into existing farming systems as conventional agricultural machinery can be used (Murphy et al., 2013). In Europe, miscanthus and switchgrass generally show better yields than reed canary grass, but in northern Europe, where cold winter temperatures are a major limitation to crop establishment and growth, reed canary grass is favored

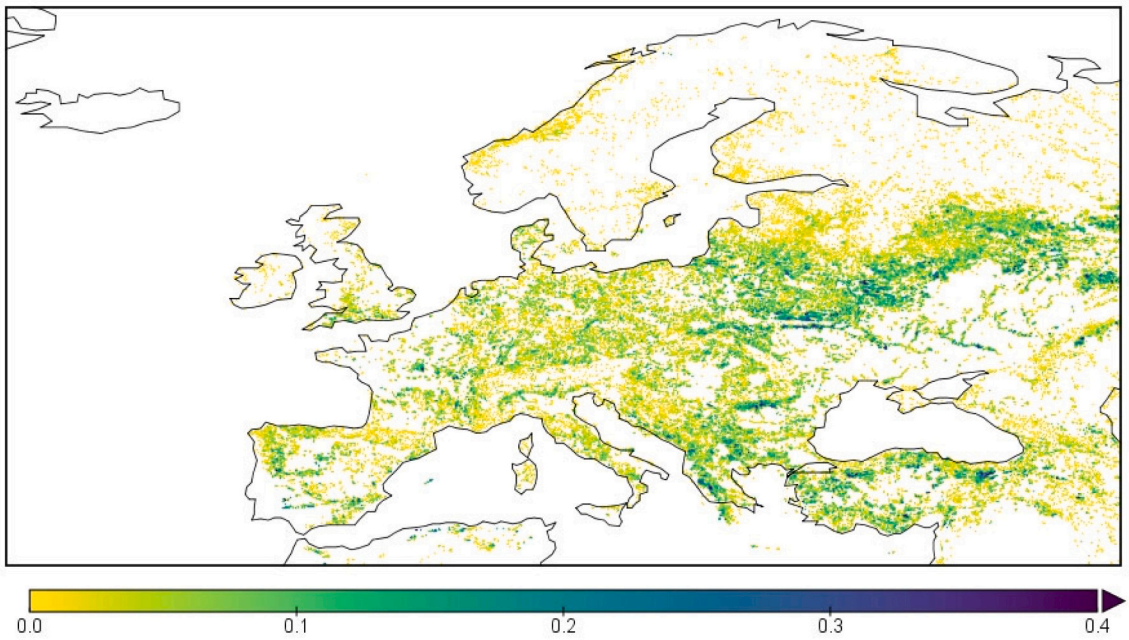

Fig. 1. Abandoned cropland in Europe from 1992 to 2015 as a fraction of a grid cell. The map retains the original horizontal resolution of the land cover data (about 300 m).

(Lewandowski et al., 2003).

Yields (lignocellulosic material, in dry mass) for the selected perennial grasses were obtained from GAEZ model version 3.0 (IIASA/FAO, 2012; Fischer et al., 2012). This model has been widely used to model attainable yields, yield gaps (Alcamo et al., 2007; Davis et al., 2017; Xu et al., 2017) and water consumptions from irrigation (Staples et al., 2013; Næss et al., 2021) for a variety of crops. More recently, the model has been applied to estimate bioenergy potentials at a global level (Staples et al., 2017; Liu et al., 2018; Næss et al., 2021), and in Europe (Van Duren et al., 2015). GAEZ allows to compute yields using three different agricultural management intensities: low, medium and high. In this work, we only use the high intensity level to better represent the dominant agricultural practices in Europe (Maggi et al., 2019; Potter et al., 2010). The yields are estimated under today's climatic conditions using mean annual values for the period 2010–2040 from Hadley Centre coupled model (HadCM3 – B1) (Lowe, 2005).The geo-referenced global climate data comprise precipitation, temperature, wind speed, sunshine hours and relative humidity, in addition to soil and terrain data. Two alternative water supply scenarios are considered, rainfed and irrigated. Crop suitability and yields in each grid cell is calculated according to 5 main steps (Fischer et al., 2012): i) climate data analysis and compilation of general agro-climatic indicators; ii) yield calculation based on crop-specific agro-climatic assessment and water-limited biomass; iii) yield-reduction due to agro-climatic constraints; iv) edaphic assessment and yield reduction due to soil and terrain limitations; v) integration of results from the 4 previous steps. The yields produced from GAEZ are then converted to primary energy potentials using lower heating values (LHV) for each specific perennial grass: 18.55 MJ kg_{DM}^{-1} for miscanthus, 18.06 MJ kg_{DM}^{-1} for reed canary grass, and 17.82 MJ kg_{DM}^{-1} for switchgrass (TNO, 2020). In addition to the cases with the three single perennial grasses, two additional cases for optimal crop mix are produced where to each grid cell is assigned the type of grass that can achieve the largest yields in both rainfed and irrigated conditions.

2.2. Life cycle assessment

The spatially explicit environmental performances for the production of miscanthus, switchgrass and reed canarygrass grown on abandoned cropland in Europe are assessed by using a life cycle perspective. The relationship between the spatial variability of bioenergy yields and environmental impacts of agricultural production is explored using updated impact assessment methods recommended by the UNEP/SETAC (Jolliet et al., 2018; Frischknecht and Jolliet, 2016).

Fig. S1 in the Supplementary Information (SI) shows a simplified flow diagram of the system boundaries and main steps for the biomass production alternatives. The system boundaries include all processes required for biomass planting, cultivation, harvesting and transport up to the farm gate. The foreground system includes on-field agricultural processes (i.e., mowing, ploughing, planting, weeding, fertilizer application, bailling, cutting) while material and energy inputs to the product system are included in the background system and modelled using the ecoinvent dastabase v.3.5 (Wernet et al., 2016). Infrastructure (such as agricultural machinery and buildings) is not included in the inventory as it generally has low contributions to the total impacts (Nemecek et al., 2007).

A crop-specific life cycle inventory (LCI) was compiled for the production of miscanthus, reed canary grass and switchgrass under both irrigated and rainfed water supply regimes. These LCIs are grid-specific as inputs such as fertizilier use, pesticides, and energy consumption for soil preparation, planting, and harvesting depend on the local yields. A crop cycle of 15 years is assumed for the three pererenial grasses. For the cases under irrigated conditions, site-specific water stress levels are explicitly considered to be mitigated by irrigation requirements, with the associated water and energy consumption attributed to the irrigation process. The average yearly agricultural operations for one hectare of cultivated land are given in Table S1-S3 in Supplementary Information for each of the perennial grasses. These values were computed from the total number of operations over the lifetime of the stand and discounted by the number of years of the crop cycle (15 years) based on the reviewed literature (see Supplementary Table S1). Fuel consumption and machinery characteristics for field operations values used in this study are available in SI (Tables S4-S8).

Nitrogen (N), phosphorus (P) and potassium (K) fertilizer application rates are the sum of the nutrients removed with the harvested biomass plus the following losses: 18% of N losses due to volatilisation and leaching (Eggleston et al., 2006), 15.8% of P losses to reflect average soil

erosion rates in Europe (Alewell et al., 2020) and 20% losses of K due to plant uptake inefficiencies (Majumdar et al., 2021). Annual nutrient removals are computed as the product between the harvested biomass and its nutrient content, and are therefore site-specific. Biomass nutrient contents are derived from the literature and are shown in Table S9 in the Supplementary Information (Kiesel et al., 2016; Oliveira et al., 2017). N, P and K are applied as urea, diammonium phosphate and potassium chloride, respectively. The nitrate leaching rate and nitrous oxide emission factors induced by N fertilizers are shown in Table S10-S11. Both direct and indirect emissions to soil, air, and water body for supply of material and energy inputs required for the different agricultural operations are considered through compilation of spatially explicit inventories. The pesticides considered in this work are herbicides, as very few pests other than weeds have been identified as potential threat to the three perennial grasses (Dubis et al., 2019; Oliveira et al., 2017; Wagner et al., 2017). Assumptions on chemical product and application rates are available in Table S12 in Supplementary Information.

2.3. Soil organic carbon (SOC) changes and integration with climate metric

Soil organic carbon changes after establishment of perennial grasses are modelled and quantified separately from the rest of the inventory. Stock changes are modelled for a soil depth of 100 cm and at a spatial resolution of 5 arcminutes. Data from the European Soil Data Center (ESDAC) (Hiederer and Köchy, 2011) are used to map the initial carbon stock for the abandoned cropland identified as suitable for production of the three perennial grasses (see Fig. S2 in Supplementary Information). SOC changes due to conversion of cropland to perennial grasses are estimated using a regression model based on a set of key site-specific climatic parameters, such as temperature, soil clay content and bulk density (Ledo et al., 2020) (see Eq.S1 in SI). The model used a harmonized global dataset of empirical values of SOC for different types of perennial crops (perennial grasses, palms, and woody plants) and produced the relative change in SOC between two measurements times. A model fit is used to explain and predict changes in SOC stocks with the most significant explanatory variables: climatic conditions (mean annual temperature, annual accumulated precipitation, climatic water deficit); topography (elevation, slope, aspect, and roughness); soil parameters (bulk density, percent clay, percent silt, percent sand, and pH); and plantation parameters (crops age, years since transition to perennials, previous and current land use) (Ledo et al., 2019).

Site specific mean annual temperature for Europe is obtained from Hadley Centre coupled model (HadCM3) (Gordon et al., 2000). We use here the mean annual for the period 2010–2040 (B1) (Lowe, 2005) for consistency with the climatic data used to model crop yields with GAEZ. Soil bulk density and clay content maps are obtained from the World Soil Information and from the International Science Council (ISC) World Data System (ISRIC, 2017) (see Supplementary Information Fig. S3–4). We then compute the SOC changes over the entire period of 15 years (crop cycle) by multiplying the grid specific SOC changes and the grid specific initial carbon stock (in t C/ha) for each grid cell (see Eq. S2 in SI). The number of grid cells suitable for cultivation vary with the perennial grasses and irrigation conditions.

Since the SOC changes are distributed over time, approaches have been proposed for a consistent inclusion of this temporal variability in the LCA framework (Petersen et al., 2013; Goglio et al., 2015). In this work, we use an approach that integrates the temporal distribution of the changes of SOC with the global C cycle to obtain specific metrics that can include distributed emissions within climate change impacts used in LCA. The method has been widely used to estimate the fraction of biogenic CO_2 fluxes remaining in the atmosphere and associated GWP factors (Cherubini et al., 2012; Iordan et al., 2018; Cherubini et al., 2016b). For each grid, the temporal profiles of the changes in SOC are integrated through a mathematical convolution with the impulse response function (IRF) of CO_2, which is a simplified carbon-cycle climate model considering the interactions of the atmosphere with the ocean and the biosphere (see Eq.S3 in SI). The IRF used is the multi-model mean consistent with the one used by the IPCC in the calculation of emission metrics (Joos et al., 2013) (described in Eq.S4 in SI). The resulting function is then included within the equation of Global Warming Potential (GWP) to compute the SOC-specific characterization factors (GWP_{SOC}) as shown in Eq.S5 in SI. The average of this factor is 0.95 ± 0.001. GWP_{SOC} takes into account the temporal profile of the CO_2 sequestration in the soil, which is distributed over 15 years, while the TH remains fixed at 100 years (hence the factors are smaller than 1). The climate change effects are then computed by multiplying the GWP_{SOC} by the changes in SOC (in t CO_2/ha) in each grid cell (see Eq.S6 in SI).

2.4. Environmental impact assessment

Our selection of environmental impact categories considers the key impacts commonly addressed in the environmental analysis of agricultural systems (Li et al., 2021; Serra et al., 2017): climate change (CC), terrestrial acidification potential (TA), marine eutrophication (ME), freshwater eutrophication (FE), fossil resource scarcity (FRS) and the water scarcity footprint (WSF). For CC, different climate metrics with a time horizon (TH) of either 20 or 100 years are used and variability on the results is tested in a sensitivity analysis.

Many LCAs usually account for climate change impacts from well mixed greenhouse gases (WMGHGs) only. These gases are CO_2, N_2O, CH_4 and other fluorinated or chlorinated gases that have a lifetime long enough that they become well mixed in the atmosphere following an emission. Their impact on climate is thus insensitive to the emission region. Our CC analysis also includes emissions of near-term climate forcers (NTCFs) like ozone precursors and aerosols, whose explicit consideration in LCA is increasingly discussed and recommended (Jolliet et al., 2018; Cavalett and Cherubini, 2018; Cherubini et al., 2016a). Many NTCFs are typically emitted by combustion processes and have a very short lifetime (from few days to a few months). They do not become well mixed in the atmosphere, so their impact depends to a large extent on the emission region and are affected by larger uncertainty than WMGHGs. Some of these species are cooling agents, such as SOx and organic carbon (OC) that scatter solar radiation, while other aerosols like black carbon (BC) are powerful warming agents, although for a short time. Other species such as carbon monoxide (CO), non-methane volatile organic compounds (VOCs) and NOx contribute to multiple climate change processes in the atmosphere, including ozone (a greenhouse gas) formation in the troposphere. As their impact depends on the emission location, both global and regional (e.g., from EU) emission metrics are available for NTCFs.

The CC characterization factors are taken from the fifth IPCC assessment report for NTCFs using maximum, minimum and average values (see Supplementary Table S13), according to the approach of the UNEP-SETAC Life-Cycle Initiative (Jolliet et al., 2018). The impacts calculated by using the minimum values for the emission metrics of NTCFs are identified as the “best case scenarios”, representative of the minimum warming potential (or maximum cooling, in the case of cooling agents like SOx and OC). On the other hand, the “worst case scenarios” are based on the maximum values for the NTCFs, representing the maximum warming potential (or minimum cooling). A suite of different emission metrics is applied to capture different aspects of the climate system responses to emissions, namely the Global Warming Potential (GWP) and the Global Temperature change Potential (GTP), both with a TH of 20 or 100 years. GWP is a metric defined as the time-integrated radiative forcing of a pulse emissions until a TH divided by an equivalent integration for CO_2. GTP is a metric that measures the change in global surface temperature at the chosen TH following an emission pulse relative again to CO_2 (Myhre et al., 2013) (see Tables S14 for the characterization factors of the WMGHGs). The life cycle emission inventories include emissions of both WMGHGs and NTCFs. Emissions of OC and BC were derived from the emissions of particulate matter (PM)

based on the methodology described in (Bond et al., 2004) (see Supplementary Table S15).

We calculate the water scarcity footprints with AWARE (Available Water Remaining) characterization factors as per the Water Use in LCA (WULCA) (Frischknecht and Jolliet, 2016, Boulay et al., 2018). We use annual country specific characterization factors for agricultural products for both irrigated and non-irrigated conditions. We compute the water scarcity footprint for each of the three perennial grasses and the optimal crop mix and for each water supply regime by multiplying the site specific m^3 water consumed per kg dry matter by the AWARE annual characterization factor for agricultural products and for the corresponding water regime (irrigated or rainfed). The country specific CF factors used in our assessment are provided in the Table S16. For example, the world average AWARE CF for irrigated agricultural products is 46 world m^3, while the European factor is 49 world m^3 (the unit world m^3 indicates that these CFs are relative to the average m^3 consumed in the world). Among the European countries, Spain has the largest country specific factor, namely 80 world m^3, followed by Cyprus with 77 world m^3 and Greece with 69 world m^3. On the other hand, Norway, Liechtenstein and Luxembourg are the countries with the smallest average country specific CFs: 0.7, 0.9 and respectively 1 world m^3. This means that consumption of a unit of water in these three countries has less impact on water scarcity when compared to the world and European averages. Consequently, the contrary is valid for Spain, Cyprus and Greece.

For the other impact categories (TA, ME, FE, FRS), characterization factors are retrieved from the ReCiPe life cycle impact assessment method (Huijbregts et al., 2016), and the LCA software SimaPro was used to operationalize the results for each impact category per kg DM of biomass. This was then translated to spatially explicit impact results using grid-specific crop yields.

3. Results and discussion

3.1. Bioenergy potentials on abandoned cropland in Europe

Table 1 shows the suitable land, yields, and total bioenergy potentials for the three perennial grasses and the energy-based optimal crop mix under rainfed and irrigated water supply. The spatial distribution of the biomass yields is shown in Fig. 3.

Under rainfed conditions, reed canary grass is the perennial grass that can be grown on the largest extension of land (14 Mha, 88% of the total abandoned cropland), followed by switchgrass (12 Mha, 72%) and miscanthus (9 Mha, 54%). Irrigation increases land suitability for all grasses up to about 95% (15 Mha) of the total available abandoned cropland (16.2 Mha). The increase in the suitability area with irrigation for reed canary grass is relatively small, from 88% to 94%. This is mostly due to the already high resilience of this perennial grass to drought conditions. On the other hand, miscanthus is showing the largest expansion under irrigation, from an initial 54% (9 Mha) to an almost 95% (15 Mha) of the total suitable abandoned cropland. The optimal crop mix can achieve the largest suitability area (15 Mha, 95%) under rainfed conditions. Out of the total 16.2 Mha of the identified abandoned cropland, only 1.1 Mha are unsuitable for bioenergy production under rainfed conditions.

For the three perennial grasses, the total biomass yield potentials are the highest for switchgrass and the lowest for miscanthus under both water supply regimes. For rainfed conditions, average biomass yields range between 7 and 15 t_{DM} ha^{-1} yr^{-1} while for irrigated conditions they almost double, ranging between 13 and 24 t_{DM} ha^{-1} yr^{-1}. On average, miscanthus, switchgrass and reed canary grass yields increase with the use of irrigation by 97%, 62% and 29%.

Across Europe, miscanthus and reed canary grass generally show relatively homogeneous yields under rainfed conditions, while it is not the case for switchgrass (with maximum values achieved between 40° and 50° latitude north). Irrigation changes both yield and crop suitability patterns in Europe (Fig. 2), as all three perennial grasses show a latitudinal pattern with homogeneous high yields in the south and decreasing yields towards higher latitudes. Overall, results show that the benefits from irrigation are two-fold: higher yields and expansion of areas suitable for farming.

There are differences in terms of bioenergy potentials and their distributions over abandoned cropland in Europe. Fig. S5 in Supplementary Information shows the annual bioenergy potentials (in GJ ha^{-1} yr^{-1}) for all three perennial grasses and the optimal crop mix under both rainfed and irrigation conditions. Overall, annual bioenergy potentials range from 1 EJ to about 7 EJ in Europe. The smallest potentials are observed for miscanthus under both rainfed and irrigated conditions, whereas switchgrass can produce up to 6.6 EJ yr^{-1} under irrigated conditions. Reed canary grass usually falls in between, and, despite it has the largest suitable area without irrigation (14.3 Mha), the associated potential (2.8 EJ yr^{-1}) is smaller than that of switchgrass (3.1 EJ yr^{-1} on 11.7 Mha). The optimal crop mix with irrigation can produce the maximum bioenergy potential (about 7 EJ yr^{-1}). This corresponds to about 10% of the total primary energy consumption in Europe (70 EJ in 2017) and almost 92% of the total European primary bioenergy supply (7.5 EJ for same year) (IEA, 2019).

There are different contributions from perennial grasses to the optimal crop allocation per grid cell, depending on the water supply alternative. In rainfed conditions, switchgrass is the most important (67%), followed by reed canary grass (30%) and miscanthus (3%). Under irrigated conditions, the relative importance of switchgrass increases, almost completely dominating (95%) the total suitable area, with a small fraction allocated to reed canary grass (1.4%) and miscanthus (4%). There is a clear latitudinal pattern for the geographical distribution of the perennial grasses in the optimal crop mix (see Fig. S6 in Supplementary Information). Miscanthus is the most suitable perennial grass at the southern edges of Europe (west and south of Portugal, south and East coast of Spain and south Italy). Switchgrass largely dominates the central area of Europe. Reed canary grass is mostly

Table 1
Overview of suitable land areas, yields and total European bioenergy potentials from perennial grasses on abandoned cropland. "Optimal crop mix" indicates the case where the perennial grass with the highest yield is selected for each grid cell. Spatial variability ranges are given with one standard deviation around the mean.

	Switchgrass		Reed canary grass		Miscanthus		Optimal crop mix	
	Rainfed	Irrigated	Rainfed	Irrigated	Rainfed	Irrigated	Rainfed	Irrigated
Suitable land [Mha]	11.7	15.4	14.3	15.2	8.8	15.3	15.1	16.1
Total harvested biomass [Mt_{DM} yr^{-1}]	174	369	155	215	60	205	205	389
Average yield [t_{DM} ha^{-1} yr^{-1}]	14.8 ±3.8	23.9 ±4.8	10.9 ±2.3	14.1 ±2.3	6.8 ±3.1	13.4 ±6.4	13.4 ±4.2	22.5 ±6.1
Total bioenergy potential [EJ yr^{-1}]	3.1	6.6	2.8	3.9	1.1	3.8	3.7	6.9
Average bioenergy potential [GJ ha^{-1} yr^{-1}]	264 ±67	428 ±86	197 ±41	255 ±41	126 ±58	249 ±119	244 ±75	431 ±109

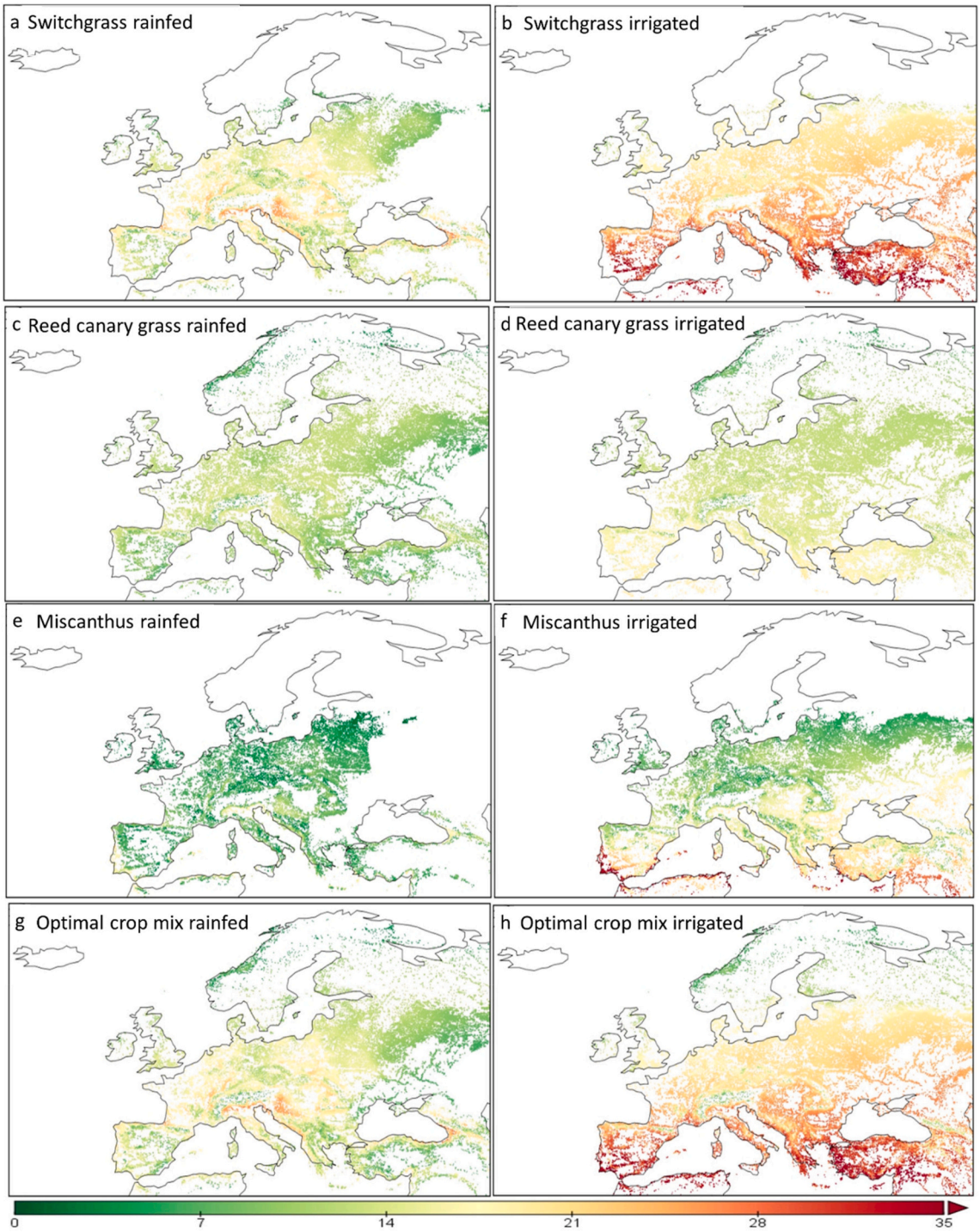

Fig. 2. Annual yields (in t_{DM} ha^{-1}) for switchgrass (a-b), reed canary grass (c-d), miscanthus (e-f), and the optimal crop mix (g -h). a,c,e,g are yields under rainfed conditions, b,d,f,h under irrigation.

predominant in northern and eastern Europe and mountainous areas, due to its C3 photosynthetic pathway that thrives better in cold and moist conditions.

3.2. Life-cycle climate change effects

Table 2 shows the aggregated characterized impacts on climate change (CC) measured in GWP100 including both life cycle emissions and soil organic carbon changes (specifically discussed in a section below). CC impacts normalized per land area range from 1.1 t CO_2eq. ha^{-1} (miscanthus under rainfed conditions) to 5.2 t CO_2eq. ha^{-1} (switchgrass with irrigation). Irrigation causes the largest increases in impacts for miscanthus (190%), followed by switchgrass (100%) and reed canary grass (71%). Under rainfed conditions, reed canary grass has the largest average and total impacts, followed by switchgrass and miscanthus.

Under rainfed conditions, the smallest impacts on CC are from miscanthus (10 Mt. CO_2eq. yr^{-1}), followed by switchgrass (31 Mt. CO_2eq. yr^{-1}) and reed canary grass (34 Mt. CO_2eq. yr^{-1}). When irrigation is considered, switchgrass becomes the most carbon intensive option (84

Table 2
Impacts on climate change (GWP100) from the production of perennial grasses under both rainfed and irrigated conditions, with a breakdown on life cycle emissions and soil organic carbon (SOC). The table shows total and average impacts according to different functional units. "Optimal crop mix" indicates the case where the perennial grass with the highest yield is selected for each grid cell. Spatial variability ranges are given with one standard deviation around the mean. Negative SOC changes represent sequestration of atmospheric CO_2.

		Switchgrass		Reed canary grass		Miscanthus		Optimal crop mix	
		Rainfed	Irrigated	Rainfed	Irrigated	Rainfed	Irrigated	Rainfed	Irrigated
Life-cycle									
	Total [Mt CO_2 eq. yr^{-1}]	31	84	34	66	10	51	38	89
	Average [tCO_2 eq. ha^{-1} yr^{-1}]	2.6 *± 0.6*	5.2 *±1.7*	2.4 *± 0.5*	4.1 *± 1.2*	1.1 *± 0.4*	3.2 *± 1.8*	2.5 *± 0.6*	5.1 *± 1.9*
	Average [kg CO_2 eq. t_{DM}^{-1}]	177 *± 4*	220 *±28*	223 *± 6*	294 *± 53*	169 *± 21*	244 *±46*	193 *± 26*	223 *± 29*
	Average [gr CO_2 eq. MJ^{-1}]	9.9 *± 0.2*	12.3 *±1.6*	12.3 *± 0.3*	16.3 *±2.9*	9.1 *± 1.1*	13.2 *± 2.5*	10.8 *± 1.4*	12.5 *± 1.6*
SOC									
	Total [Mt CO_2 eq. yr^{-1}]	−47	−59	−58	−60	−33	−56	−59	−61
	Average change rate [%]	13.3% *±5.1*	13.4% *±5.1*	14.1% *±5.4*	13.9% *±5.4*	12.2% *±5.1*	12.7% *±5.2*	13.7% *±5.7*	13.4% *±5.7*
	Annual stock change [t CO_2 ha^{-1} yr^{-1}]	−4.5 *±7.3*	−4.3 *±6.9*	−5.1 *±8.1*	−4.9 *±7.9*	−4.1 *±6.7*	−3.9 *±6.3*	−4.9 *±8.0*	−4.7 *±7.8*
Net CC impact									
	Total [Mt CO_2 eq. yr^{-1}]	−16	25	−24	6	−23	−5	−21	28
	Average [t CO_2 eq. ha^{-1} yr^{-1}]	−1.9 *±1.4.*	0.9 *±0.8*	−2.7 *±1.5*	- 0.8 *±0.01*	−3 *±1.6*	−0.7 *±0.6*	−2.4 *±0.7*	0.4 *±0.2*

Mt. CO_2eq. yr^{-1}), followed by reed canary grass (66 Mt. CO_2eq. yr^{-1}) and miscanthus (51 Mt. CO_2eq. yr^{-1}). On the other hand, when comparing the relative change from rainfed to irrigated conditions, miscanthus has the largest increase (about 5-fold) in CC impact, followed by switchgrass and reed canary grass (which nearly doubles). This increase is mostly driven by energy required for irrigation processes, which can represent a large share of the total annual CC impact: 21% for miscanthus, 14% for reed canary grass and 12% for switchgrass (Fig. S7 Supplementary Information).

The major stages contributing to life-cycle emissions under rainfed conditions are N fertilizers (75% for switchgrass, 77% for reed canary grass, and 56% for miscanthus), harvesting operations (10% for switchgrass, 8% for reed canary grass, and 22% for miscanthus) and K fertilizers (2% for switchgrass, 3% for reed canary grass, and 4% for miscanthus). When irrigation is included, the major step contributing to total emissions is still N fertilizer (59% for switchgrass, 56% for reed canary grass, and 36% for miscanthus), but water supply processes (both machinery and energy consumption) also become a relevant share (24% for switchgrass, 28% for reed canary grass, and 41% for miscanthus).

With the optimal crop mix, the total annual CC impacts from life-cycle emissions are 10% larger than the highest impact of the individual grass in rainfed conditions and 6% larger in irrigated conditions. However, the normalized average CC impacts per hectare of land, dry matter, and unit of energy are smaller than the largest individual perennial grass emissions for both water supply regimes. One unit of energy (1 MJ) produced from the optimal crop allocation under irrigated conditions has an emission of 10.8 g CO_2eq., an increase of 19% and 20% relative to switchgrass and miscanthus, respectively, and a decrease of 14% relative to reed canary grass.

Regional variabilities from life-cycle CC impacts show similar patterns for all three perennial grasses when comparing rainfed and irrigated conditions (Fig. 3). The pattern under irrigated scenarios is similar for the different crops, with the largest impacts in more arid areas such as southern and eastern Europe, which would require relatively higher irrigation levels.

Our findings regarding impacts per unit of dry matter are broadly consistent with those reported in the literature (Murphy et al., 2013; Kiesel et al., 2016; Sanscartier et al., 2014). CC impacts were found to vary between 40 and 170 kg CO_2 eq. t_{DM}^{-1} for miscanthus grown under rainfed conditions (Sanscartier et al., 2014; Robertson et al., 2017a; Krzyżaniak et al., 2020). Impacts on CC from cultivation of miscanthus in a low fertility site in Poland vary between 34 kg CO_2 eq. t_{DM}^{-1} when grown without fertilization up to 675 kg CO_2 eq. t_{DM}^{-1} when a mix of fertilizers is used (Krzyżaniak et al., 2020). The main reasons for the large ranges are variations in yields, land use efficiency as well as crop cycle lengths. Similar to our findings, fertilization and harvesting operations are generally found to be the processes with the highest emissions across the life cycle (Perić et al., 2018; Krzyżaniak et al., 2020; Tadele et al., 2019). The environmental performance of the agricultural production of switchgrass grown under rainfed conditions ranges from 83 to 145 kg CO_2 eq. t_{DM}^{-1} (Kiesel et al., 2016; Brassard et al., 2018), with N emissions having the largest contribution (Ashworth et al., 2015). CC impacts for switchgrass under irrigated conditions were reported to be up to 700 kg CO_2 eq. t_{DM}^{-1} for a location in Spain, an area particularly dry where irrigation accounted between 50 and 80% of the total impacts (Escobar et al., 2017). The reported environmental impacts of switchgrass are generally higher than those of miscanthus (Kiesel et al., 2016; Smeets et al., 2009), a trend consistent with our results. This can primarily be attributed to the larger potential yields at lower fertilizer requirements in the case of miscanthus (Smeets et al., 2009; Kiesel et al., 2016).

3.3. Changes in soil organic carbon (SOC)

There is high variability across Europe for the initial SOC stocks of cropland (Fig. S2 in Supplementary Information). Values range between 66 and 4334 t CO_2ha^{-1}, with the largest initial stocks in north-eastern Europe. The annual average SOC changes in Europe under rainfed conditions are the largest for reed canary grass (58 Mt. CO_2eq.yr^{-1}), followed by switchgrass (47 Mt. CO_2eq.yr^{-1}) and miscanthus (33 Mt. CO_2eq.yr^{-1}) (see Table 2). With irrigation, the differences among the three perennial grasses are smaller: 60 Mt. CO_2eq.$yr^{-1}$for reed canary grass, 59 Mt. CO_2eq.yr^{-1} for switchgrass, and 56 Mt. CO_2eq.$yr^{-1}$for miscanthus. Note that the difference between rainfed and irrigated conditions only affects the extension of the suitable areas for the different crops, which vary in terms of initial SOC and accumulation rates. Under irrigation conditions, almost the entire available abandoned cropland area is suitable for the agricultural production, thereby

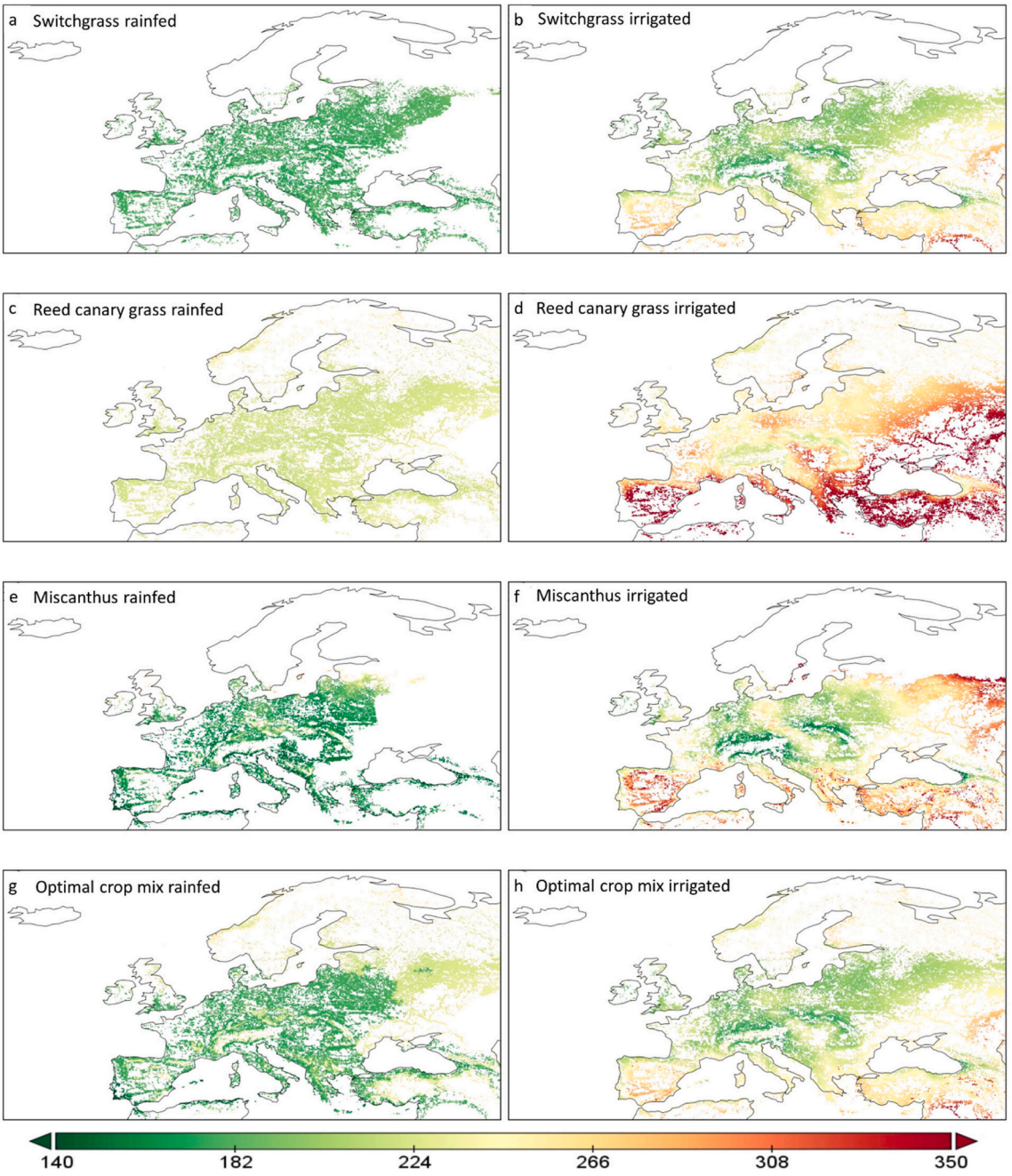

Fig. 3. Impacts on climate change from life-cycle emissions (computed with GWP100) in kg CO_2eq. t_{DM}^{-1} for switchgrass (a-b), reed canary grass (c-d), miscanthus (e-f), and the optimized allocation of crops based on the maximum energy output per grid (g -h). In figures a, c, e and g are yields under rainfed conditions while in b, d, f and h with irrigation. Note the differences in the scales of the color bars in the different panels.

increasing the carbon sequestration potential in European soils.

Fig. 4 shows the spatial distribution of the average SOC rate changes (%) across the 15 years of crop cycle under rainfed conditions. All crops present almost the same latitudinal pattern with increasing SOC accumulation rates towards the northern part of Europe. The lower range of SOC rates (below 10%) are mainly located in the southern areas of the continent. The averages of annual SOC stock changes are the highest for reed canary grass (5.1 $tCO_2eq.ha^{-1}$), followed by switchgrass (4.5 $tCO_2eq.ha^{-1}$) and miscanthus (4.1 $tCO_2eq.ha^{-1}$). For the optimal crop mix scenarios, the total annual SOC changes are similar to the largest value from the three perennial grasses, namely the reed canary grass.

Our estimates of SOC changes are broadly in line with results from previous studies. A global meta-analysis that assessed land transitions from cropland to switchgrass and miscanthus found average SOC increasing rates between 10% - 15% (Qin et al., 2016). There is usually larger variability among grass types (1.83 t CO_2 ha^{-1} and 7.83 t CO_2 ha^{-1}) than what is found in our study (3.9 t CO_2 ha^{-1} and 5.1 t CO_2 ha^{-1}). This can be explained by the global scope of the meta-analysis, while our analysis focuses on Europe only. Further, the method used in our analysis does not distinguish SOC changes by specific grass types (Ledo et al., 2020), thereby potentially favoring average changes over outliers.

3.4. Net climate change effects

The net annual CC impacts, calculated as the sum of the CC impacts from life-cycle emission and SOC changes, are negative for all crops under rainfed conditions. This means that perennial grasses on

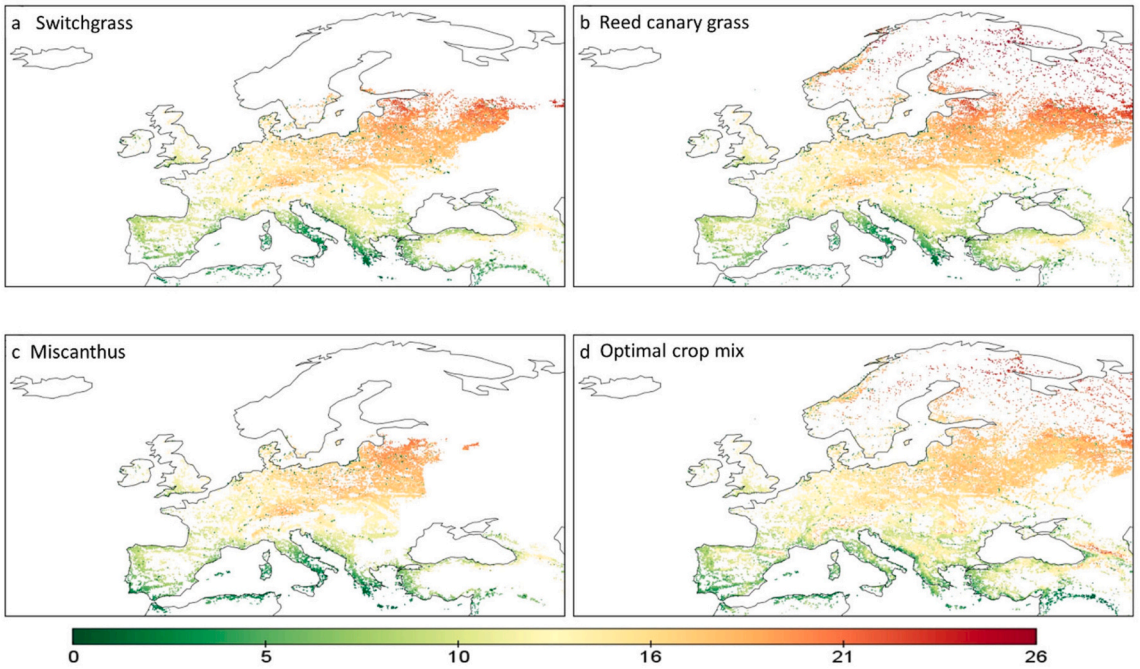

Fig. 4. Spatial explicit average increasing rates (%) of changes in soil organic carbon for three perennial grasses and the optimized crop mix under rainfed conditions where: a) switchgrass, b) reed canary grass, c) miscanthus and d) optimal crop mix.

abandoned agricultural land can absorb more CO_2 into the soil than the GHGs released during their agricultural production and have potential to contribute to negative emissions while delivering an energy source. Reed canary grass has the largest annual net negative emissions (−24 Mt. CO_2eq.yr^{-1}), followed by miscanthus (−23 Mt. CO_2eq.yr^{-1}) and switchgrass (−16 Mt. CO_2eq.yr^{-1}). Under irrigated conditions, annual climate impacts turn to positive for switchgrass (25 Mt. CO_2eq.yr^{-1}) and reed canary grass (6 MtCO_2 eq. yr^{-1}), while they remain negative for miscanthus (−5 MtCO_2eq. yr^{-1}). In terms of normalized results, the annual average net negative emissions under rainfed conditions are the largest for miscanthus (−3 t CO_2eq.ha^{-1}), followed by reed canary grass (−2.7 t CO_2eq.ha^{-1}) and switchgrass (−1.9 t CO_2 eq. ha^{-1}).

Table 3
LCA results for the impact categories TA (terrestrial acidification), FE (freshwater eutrophication), ME (marine eutrophication), FRS (fossil resource scarcity) and WSF (water scarcity footprint) for all three considered perennial grasses and the optimal crop mix. Spatial variability ranges refer to one standard deviation around the mean.

		Switchgrass		Reed canary grass		Miscanthus		Optimal crop mix	
		Rainfed	Irrigated	Rainfed	Irrigated	Rainfed	Irrigated	Rainfed	Irrigated
TA	**Total** [10^6kg SO_2 eq. yr^{-1}]	630	1421	725	1084	155	619	781	1486
	Average [kg SO_2 eq. t_{DM}^{-1}]	3.6 ± 0.01	3.9 ±0.1	4.7 ±0.01	5 ±0.2	2.2 ±0.1	3 ±0.2	4 ±0.6	3.9 ±0.3
	Average [kg SO_2 eq. TJ^{-1}]	204 ±0.5	214 ±7.1	259 ±0.8	276 ±13	141 ±3.4	160 ±11	222 ±30	217 ±18
FE	**Total** [10^6 kg P eq. yr^{-1}]	7	24	8	22	4	23	8	26
	Average [g P eq. t_{DM} $^{-1}$]	37 ±7.8	66 ±18.2	49 ±11.7	101 ±35	68 ±38	113 ±33	44 ±14.3	64 ±20
	Average [kg P eq. TJ^{-1}]	2.2 ±0.4	3.4 ±1.0	2.8 ±0.7	5.2 ±1.9	4.6 ±2.0	6.2 ±1.8	2.5 ±0.8	3.6 ±1.1
ME	**Total** [10^6 kg N eq. yr^{-1}]	129	294	147	218	30	111	160	306
	Average [g N eq. t_{DM}^{-1}]	746 ±0.1	798 ±1.4	948 ±0.3	1015 ±2.5	503 ±1.5	540 ±2.2	813 ±109	805 ±73
	Average [kg N eq. TJ^{-1}]	42 ±0.01	45 ±0.1	52.5 ±0.02	56.2 ±0.1	27.1 ±0.1	29.1 ±0.1	45 ±5.9	45 ±4.1
FRS	**Total** [Mt oil eq. yr^{-1}]	4	15	5	12	2	12	5	16
	Average [kg oil eq. t_{DM}^{-1}]	25 ±0.6	41 ±9	30 ±0.8	57 ±16.6	28 ±3.6	58 ±14.3	27 ±2.9	39 ±9.4
	Average [kg oil eq. MJ^{-1}1]	1.4 ±0.03	2.2 ±0.5	1.7 ±0.1	2.9 ±0.9	1.6 ±0.2	3.0 ±0.8	1.5 ±0.2	2.2 ±0.5
WSF	**Total** [10^9 world m^3 eq. yr^{-1}]	10	2375	11	2129	3	2649	5	2727
	Average [world m^3 eq. kg_{DM}^{-1}]	0.05	4.68	0.07	7.21	0.04	9.01	0.02	4.84

On an annual basis, the scale of negative emissions that can be achieved by growing perennial grasses on abandoned cropland in Europe ranges between −16 to −24 Mt. CO_2-eq. under rainfed conditions, and up to −5 Mt. CO_2-eq. under irrigated conditions. Considering that the total emissions of GHGs from the agricultural sector in Europe (EU-28) were about 435 Mt. CO_2-eq. yr^{-1} in 2018, the scale of negative emissions from perennial grasses corresponds to about 3.7% - 5.6% with rainfed production, and 1.2% with irrigation, of the total emissions from agriculture. These shares become nearly two times bigger if only SOC changes are considered, i.e., without the emissions from life-cycle agricultural operations (some of which are to be reported in the energy sector, and not in the agricultural sector).

3.5. LCA results for other impact categories

Table 3 shows the aggregated characterized impacts on terrestrial acidification (TA), freshwater eutrophication (FE), marine eutrophication (ME), fossil resource scarcity (FRS) and water scarcity footprint (WSF). The spatial distribution of these impacts is shown in Fig. 5 for switchgrass and in Fig. S8–9 in Supplementary Information for reed canary grass and miscanthus.

Under rainfed conditions, total impacts across all impact categories are the highest for reed canary grass, followed by switchgrass and miscanthus. With irrigation, TA for switchgrass has the largest increase (as well as the highest absolute impact), followed by reed canary grass (which has the smallest increase, about 50%), and miscanthus. The main drivers for higher TA impacts with irrigation are emissions from N fertilizers (see Fig. S7 in Supplementary Information), which are a consequence of higher yields (more N fertilizers are needed to support productivity) and water supply related inputs (machinery and energy consumption). In contrast with the total impacts, the average TA impacts per unit of biomass show relatively small variations from rainfed to irrigated conditions, with the largest increase for miscanthus (17%), followed by reed canary grass (11%) and switchgrass (7%). In the optimal crop mix scenarios, total TA impacts are higher than for the individual crops due to the larger suitable area for biomass production, but, similarly to the CC impacts, the normalized annual averages are in between the ranges of the individual crops. The spatial distribution of the TA impacts for switchgrass shows different patterns depending on water supply conditions: there are almost homogenous impacts under rainfed conditions, while under irrigation there are decreasing impacts towards the northern areas, with the maximum impacts in the southern edges of the continent (see Fig. 5 a-b).

Total impacts on FE are increasing the most for miscanthus (4 times) followed by switchgrass (2 times) and reed canary grass (1.5 times) when comparing rainfed to irrigated conditions. Crop establishment inputs are the main drivers (62%) of the total FE impact under rainfed conditions for reed canary grass, while harvesting is the largest contributor for miscanthus (81%) and switchgrass (65%). Under irrigated conditions, the largest impact comes from energy use for irrigation (54% - 60%) (Fig. S7 in Supplementary Information). The areas where the largest impacts on FE for switchgrass production occur are under rainfed conditions the north-eastern region of the continent. With irrigation, there is a more pronounced latitudinal pattern with increasing impacts towards the southern part of Europe (see Fig. 5 c-d).

In rainfed conditions, nitrogen fertilizer is the main contributor to impacts across all impact categories, except for FE. The main driver for FE is the inputs for crop establishment, notably phosphorous and nitrate emissions, for reed canary grass (62%). When irrigation is considered, the inputs for artificial water supply (irrigation machinery and energy consumption for pumps) have the largest contribution in the total impacts (Fig. S7 in Supplementary Information) for FE and FRS, while for TA and ME the nitrogen fertilizer is still the dominant driver.

Results for the water scarcity footprints range for the rainfed conditions between 0.04 and 0.07 world m^3 eq. kg_{DM}^{-1}, with miscanthus having the smallest footprint and reed canary grass the largest. For irrigated conditions, our average values are between 4.7 (switchgrass) and 9 (miscanthus) world m^3 eq. kg_{DM}^{-1}. The hot spots for the water scarcity are the southern regions of Europe with Portugal, Spain and Italy having the largest footprints. Irrigation in these areas thus has higher risks to exaggerate water scarcity issues (see Fig. S8–9).

The cases with an optimal crop mix imply that more area is under production, and therefore lager total impacts at European level. When looking at the average impacts per harvested biomass, the values are in between the minimum and maximum of those of the individual perennial grasses. This means that appropriate land management can deliver optimal bioenergy potential with no elevated impacts. Across all impact categories considered in this work, the southern regions of Europe are showing the maximum impacts under irrigated conditions. Results from this work compare well with estimated impact of miscanthus biomass production as modelled in ecoinvent version 3.5 using the same LCIA methods (Nemecek, Wernet et al., 2016). TA impacts in literature were found to vary between 0.3 and 16 kg SO_2 eq. t_{DM}^{-1} for miscanthus (Kiesel et al., 2016; Krzyżaniak et al., 2020). One reason behind the large variability in the acidification impacts is the large range of yields and fertilizer inputs reported in the studies. Previous studies agreed that N emissions have the largest contribution to TA (Ashworth et al., 2015; Kiesel et al., 2016; Krzyżaniak et al., 2020). Similar to our results (see Fig. S7 in Supplementary Information), another LCA study reported an almost 80% contribution to the ME impact from the fertilizer application (Tadele et al., 2019). Impacts on FE vary in the case of miscanthus between 3 and 250 g P eq. t_{DM}^{-1} (Krzyżaniak et al., 2020; Kiesel et al., 2016). Herbicide application and fertilization operations are generally found in other studies as well as in ours to be the processes with the largest share of impacts on the FE (Krzyżaniak et al., 2020; Perić et al., 2018). Our results for impacts on FRS are in line with estimations from previous studies which reported values between 12 and 75 kg oil eq. t_{DM}^{-1} (Krzyżaniak et al., 2020).

3.6. Sensitivity to irrigation and climate metrics

Table S17 shows the difference in impacts between irrigated and rainfed conditions across 6 impact categories and for the annual European agricultural production considering the three perennial grasses. Across all impact categories, reed canary grass has the smallest sensitivity to irrigation for the total impact values, followed by miscanthus and switchgrass. On the other hand, when looking at the normalized average values, switchgrass has the lowest difference between irrigated and rainfed conditions, apart from ME (which has N fertilizer as the main contributing process).

Climate change impacts are highly sensitive to the climate metrics considered, either GWP20, GWP100, GTP20 or GTP100, and to contributions from NTCFs when included in the analysis (Fig. S10 and Table S18 in the Supplementary Information). These different metrics refer to different types of climate impacts. GWP20 is a metric that informs about the climate change impacts in the very short-term and assigns relatively high importance to short-lived forcers such as NTCFs or CH_4. As the characterization factors for GWP100 are numerically similar to those of GTP40 (Allen et al., 2016), GWP100 can be taken as a proxy for the temperature impact occurring about four decades after the emissions. GTP100 is the metric assessing climate change impacts in a longer timeframe, as it measures the temperature changes 100 years after its emission. This is a metric that can be interpreted as a measure of long-term temperature stabilization, as advocated in the Paris Agreement (Tanaka et al., 2019).

Results computed with GWP20 are higher than those with GWP100, especially when NTCFs are included, indifferent to the type of water supply or the metric. The largest variability in absolute values is registered for GWP20 with irrigation, with the largest variation for switchgrass (140 Mt. CO_2eq. as difference between the maximum and minimum values), followed by miscanthus (120 Mt. CO_2eq.) and reed canary grass (113 Mt. CO_2eq.). This variation is due to the large

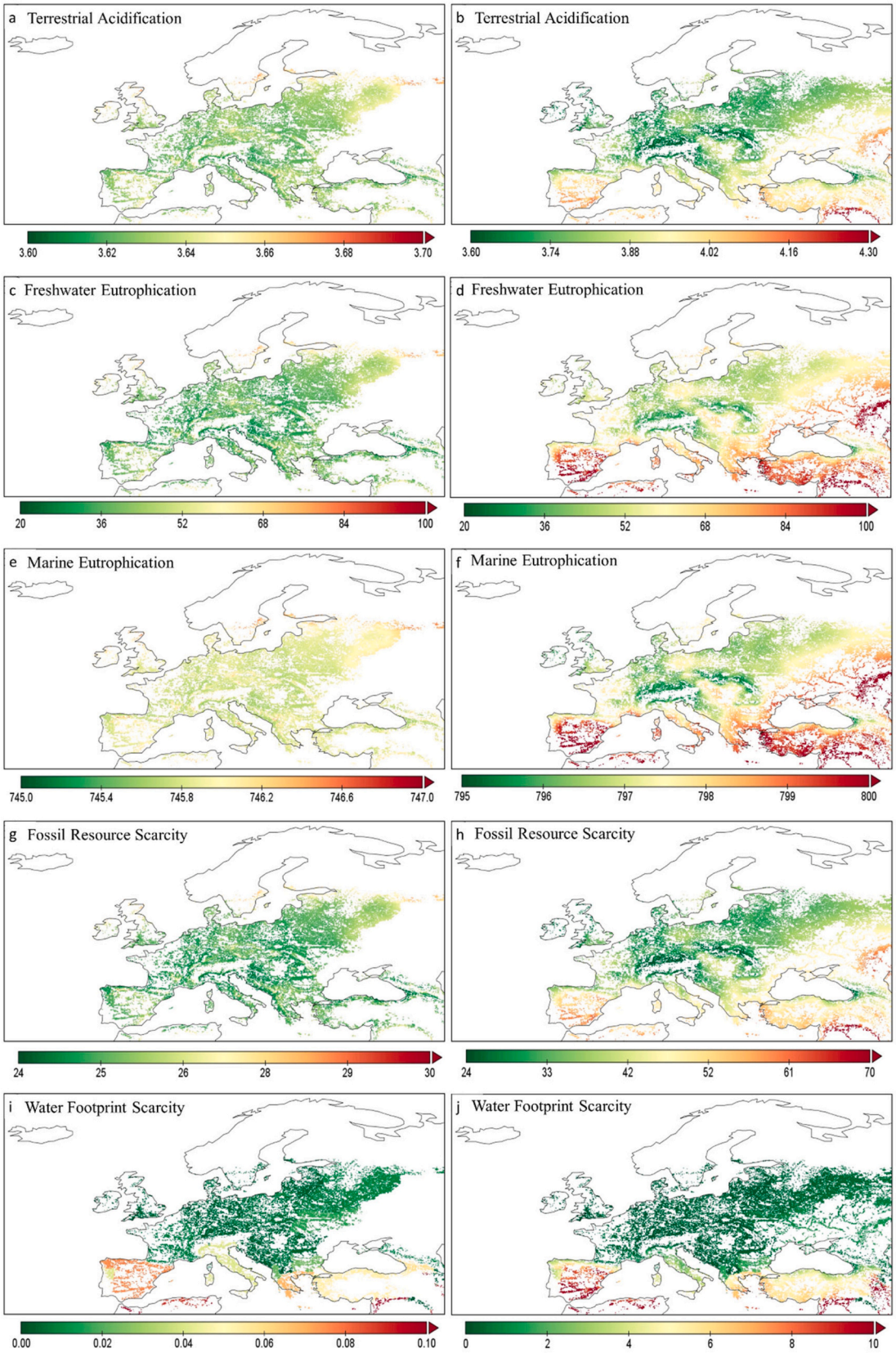

Fig. 5. Spatially explicit impacts from agricultural production of switchgrass on abandoned cropland in Europe. Results are for terrestrial acidification (a -b) in kg SO_2eq.t_{DM}^{-1}, freshwater eutrophication (c-d) in g Peq.t_{DM}^{-1}, marine eutrophication (e-f) in g N eq.t_{DM}^{-1}, fossil resource scarcity (g-h) in kg oil eq.t_{DM}^{-1} and water footprint scarcity (i-j) in world m^3eq.kg_{DM}^{-1} under rainfed (a,c,e,g,i) and irrigation (b,d,f,h,j).

differences in the estimates for NTCFs. In the minimum (best) scenario, NTCFs are negative thus having a cooling impact and compensating for some of the impact from the WMGHGs. On the other hand, at the upper end of the uncertainty range (the maximum (worst) scenario), these species can have large warming effects, with absolute values comparable with the ones from the WMGHGs (see Table S18 in Supplementary Information). Because of the longer TH of the metric, GWP100 is less sensitive to the inclusion of NTCFs than GWP20. The breakdown of the

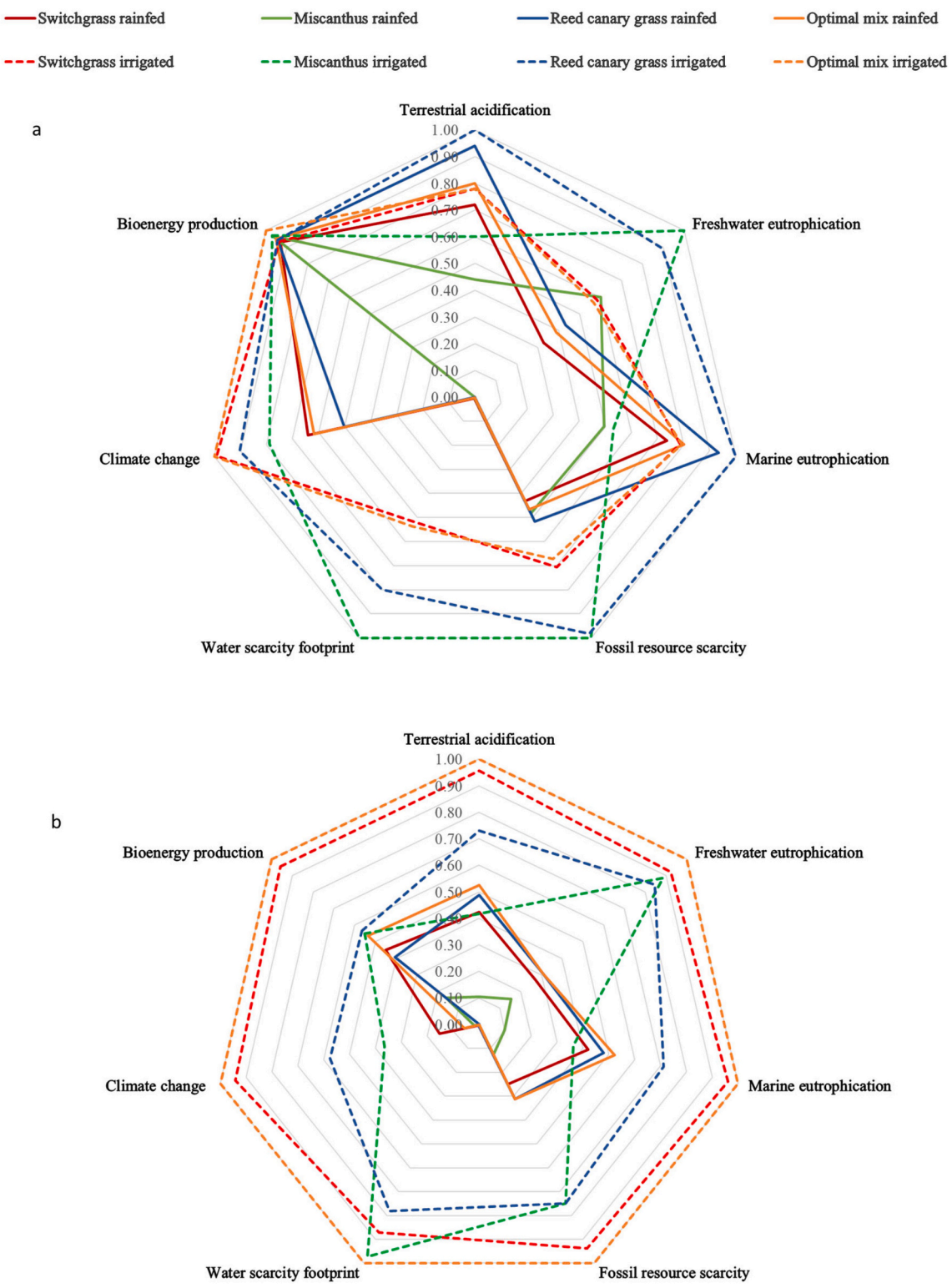

Fig. 6. Overview of co-benefits and tradeoffs of growing perennial grasses on abandoned cropland in Europe for the average (a) and total (b) scores. Solid lines show the scores for the rainfed conditions, and dashed lines for irrigated. Within each of the 6 impact categories (Terrestrial acidification, Freshwater eutrophication, Marine eutrophication, Fossil resource scarcity, Climate Change and Water scarcity footprint), the results for each of the eight scenarios are normalized relative to the highest impact, using the average results (for a) and annual total European results (for b) from Tables 3 and 4. A score of 1 indicates the worst relative performance for the environmental impacts. For bioenergy potentials, 1 indicates the maximum value.

contributions from the individual NTCFs shows that the dominant cooling driver is SOx (Table S19 in Supplementary Information), which is mostly emitted from the fertilizer production process (based on global estimates for production of phosphoric acid). Climate change effects with GTP100 are smaller than those with GWP100, because GTP100 is an instantaneous metric that only measures the temperature change at the TH and the contributions from NTCFs are negligible.

In general, no single metric can duly represent the diversity in the climate system response, and testing results across different metrics can inform of potential contrasting effects between the short and the long-term. Depending on the timeframe of interest for the climate change impacts, these complementary metrics provide information on the main GHG contributors affecting the results. Thus, for very short-term goals, the GWP20 results point to the high importance to mitigate short-lived gases as CH_4 and other NTCFs. While for long-term temperature stabilization goals, the efforts should be focused towards cutting down emissions of CO_2, the most relevant long-lived GHGs.

3.7. Co-benefits and trade-offs

Fig. 6 shows an overview of the co-benefits and trade-offs of the energy potentials and environmental impacts of growing perennial grasses on abandoned cropland in Europe for both average (Fig. 6a) and total European values (Fig. 6b). Results are based on Tables 2 and 3 and are normalized relative to the highest impact in each impact category (a score of 1 indicates the worst relative performance). Since the net climate change impacts can be negative (due to negative emissions from increases in SOC), these scores are normalized across a scale between 0 and 1 to avoid negative numbers. For bioenergy potentials, a score of 1 indicates the highest potential across the different cases.

In general, there are very large differences on the water footprints between irrigated and rainfed scenarios, given the water requirements when irrigation is considered. For European average results (Fig. 6a), the case with the highest average bioenergy potentials (optimal mix irrigated) also has the worst relative score for climate change. Miscanthus irrigated has the second highest bioenergy potential but the highest impacts across three impact categories (water footprint scarcity, fossil resource scarcity and freshwater eutrophication), and the lowest impacts on CC among the irrigated cases. Miscanthus (even with irrigation) has the lowest scores on ME and TA, well below rainfed switchgrass and reed canary grass. Reed canary grass irrigated and rainfed have the third and fourth highest bioenergy potentials, and the worst relative scores for TA and ME because of their large dependency on fertilizers. The highest results on water scarcity footprint of reed canary grass and miscanthus irrigated are due to their elevated water requirements. Switchgrass irrigated has high bioenergy potentials as well as a high score on CC, but the impacts in the other categories are relatively low. The two optimal crop mix cases usually have high bioenergy potentials and CC impacts, but lower scores in the other impact categories. These options therefore show the best balance between bioenergy production and environmental impacts, except for climate change.

The situation differs when looking at the relative performances from all the suitable land areas in Europe (Fig. 6b), as results become sensitive to the amount of area used and bioenergy production volume. The cases with the highest bioenergy potentials are also those with the worst relative performances across the different impact categories. Among the three grasses, miscanthus has a high water footprint despite the lowest yields. The bioenergy production from irrigated miscanthus is similar to that of the optimal crop mix rainfed (where switchgrass is the dominating grass), while its water scarcity footprint is similar to the optimal crop mix irrigated and the freshwater eutrophication score is similar to that of irrigated switchgrass. Switchgrass with irrigation, opposite to the trend from the average scores, has the second largest bioenergy potential as well as the second worst relative scores across all the other categories (except for WSF). Nevertheless, under rainfed conditions, switchgrass has the second-best bioenergy potential among the rainfed scenarios (behind the optimal crop mix), the worst score on CC but the lowest scores across all the other categories.

3.8. Uncertainties and limitations

In the first part of this section, the uncertainties of our approach, methods and data are reviewed. In the second part, the limitations and the aspects that have not been included in our analysis are discussed.

Our assessment is based on abandoned cropland quantified using the remotely sensed ESA CCI-LC dataset. This product has a global overall accuracy of 71%, with variations between regions and classes (Karvonen et al., 2018). Reported regional overall accuracies are 64% in Finland (Karvonen et al., 2018), 84% in coastal Eurasia (Hou and Hou, 2019), 62% in the Arctic (Liang et al., 2019), and 68–84% across different Portuguese regions (Fonte et al., 2019). Cropland classes have the highest global accuracy, with median reported user and producer accuracies across global validation efforts of 79% and 89%, respectively (Santoro et al., 2017; Tsendbazar et al., 2016; Liu et al., 2020). More refined estimates of abandoned cropland require assessments of actual land availability based on local evaluations.

The abandoned cropland identified in this work had transitions from cropland to other land cover classes, mostly forests (11 Mha) and grasslands (5 Mha). The largest extent of this transition (about 50%) occurred between 1993 and 2000 (Supplementary Fig. S11), and the transition in the last period of our assessment can include land that has been intentionally left fallow and free from agricultural production for a certain number of years. A reintroduction of these areas into active management implies some CO_2 emissions to clear the land, especially where forested vegetation has established at early stages of development. Relative to tropical land and afforestation programs, natural revegetation of abandoned areas takes place at relatively slow pace in Europe. The mean European above ground carbon sequestration rate from natural revegetation has been recently estimated at 4.55 t CO_2 ha^{-1} yr^{-1} (Cook-Patton et al., 2020). Applying this factor to the amount of land encroached by trees (about 11 Mha) times the number of years after abandonment until 2020, the total carbon sequestrated would amount to about 950 Mt. CO_2. This initial carbon penalty would not offset the benefits from SOC increase of perennial grasses, which are about 1513 Mt. CO_2.

The bioenergy potentials, together with the environmental impacts, are strongly related to yield estimates from GAEZ. Calculated yields vary across crop models based on a variety of structural differences and assumptions describing agricultural management.(Rosenzweig et al., 2014) Relative to two other crop models (Ai et al., 2020; Li et al., 2018), GAEZ shows intermediate rain-fed yields and the highest irrigated yields in Eastern Europe (Næss et al., 2022). In this work, miscanthus yields are generally lower than previously reported field observations, which range between 10 and 20 t_{DM} ha^{-1} yr^{-1} under rainfed conditions (Dubis et al., 2019; Alexopoulou et al., 2015; Borkowska and Molas, 2013), or other modelling tools such as MISCANFOR, a crop-productivity model specifically developed and calibrated for miscanthus, which predicts yields larger than 20 t_{DM} ha^{-1} yr^{-1} in most regions of Europe (Hastings et al., 2009). Commercial yields commonly achieved for switchgrass range between 10 and 13 t_{DM} ha^{-1} yr^{-1}, somewhat lower than the average European yield estimated from GAEZ. Field trials in Greece with drip irrigation and fertilization reported yields for switchgrass between 10 and 12.5 t_{DM} ha^{-1} yr^{-1}, while field trials in Italy under rainfed and unfertilized conditions reported ranges between 9 and 16.5 t_{DM} ha^{-1} yr^{-1} (Alexopoulou et al., 2020). Reed canary grass yields are previously reported to be around 8 t_{DM} ha^{-1} yr^{-1} (Powlson et al., 2005).

As an additional benchmarking investigation, we compared at the grid level the switchgrass and miscanthus annual yields from GAEZ with those from a recently produced dataset that upscaled field observations with machine-learning algorithms to produce global estimates of bioenergy crop yields (Li et al., 2020). The results of the comparison (for

which values for GAEZ are those produced under rainfed conditions and medium management intensity for better consistency) are shown in Fig. S12 in SI for the same grids of the domain of our analysis. GAEZ data are generally more conservative for miscanthus yields, while for switchgrass there is not a clear bias emerging from the cross-comparison of the two datasets. Expanding field trials and multi-model assessments under similar climatic conditions and locations of field trials can better compare, validate, and calibrate yield outcomes to improve model performances.

For water requirements, GAEZ models irrigation water volumes based on optimal management (i.e. no water deficits during growth cycle) (Fischer et al., 2012), but, in practice, water use may be higher due to sub-optimal timing or water spillage. While irrigation volumes retrieved from GAEZ are site specific, the irrigation process itself is assumed to be the same for all locations and irrigation amounts. Our inventory of irrigation was created by averaging four standard ecoinvent processes designed for France, Germany, Spain and Switzerland. Thus, processes for western Europe are assumed to be dominant in our study area, despite they might not reflect the technologies used in, e.g., eastern Europe. Another limitation is linked to the ecoinvent database itself because these processes share many common assumptions (they mainly differ for the electricity consumption per unit of water). Studies that have investigated the impact from irrigation show large spatial variation per unit of volume irrigated (Daccache et al., 2014). Differences mainly arise from the water source (groundwater or surface water) and the technology used (Daccache et al., 2014), which are both known to vary across Europe (FAO, 2017). These aspects can influence the estimates of our impacts of growing perennial grasses under irrigated conditions. The availability of grid-specific data on agricultural irrigation processes could improve the accuracy of these estimates.

An average crop cyle of 15 years is assumed in this study for all types of perennial grasses. However, earlier work indicated that productivity of a miscanthus plantation can be maintained up to 25 years (Lewandowski et al., 2003), but long-term field trials have shown a decrease in yields with stand age (Christian et al., 2008; Angelini et al., 2009). Recent work generally assumes shorter crop cycles, typically ranging between 15 and 20 years (Hastings et al., 2017). For reed canary grass, stands in Sweden had maintained yields over 16 years (Pahkala et al., 2008), while trials in Ireland have shown low stand persistence after 4 years (Finnan et al., 2016). Reported lifetimes for switchgrass plantations range from 5 to 20 years (Samson et al., 2016; Elbersen et al., 2013). The lowest estimates were reported in Canada where new diseases (head smut, anthracnos) affected the culture and are expected to increase in severity in the future as planted area increases (Samson et al., 2016). However, no serious disease has yet been reported in Europe or US and estimates for European conditions under proper management range between 10 and 20 years (Elbersen, and M., K., 2013; Smeets et al., 2009; Kiesel et al., 2016).

This work is not taking into consideration the issue of the carbon permanence in the soil. Carbon accumulated in the soil has a risk to be returned to the atmosphere in case of a future change in land management or land use (Ramesh et al., 2019), or because of enhanced respiration induced by climate change (Heikkinen et al., 2022). These aspects are highly uncertan and require speculations of future situations, which we do not include in our analysis. However, policies should be in place to secure that the gains in soil organic carbon are preserved and risks to release back CO_2 to the atmosphere reduced.

The economic aspects of bioenergy crops production have not been a focus of this work. Nevertheless, multiple integrated assessment models (IAM) show that the economic limitations of biomass feedstock availability are highly relevant, especially after 2050 (Daioglou et al., 2020). Most IAMs show that in high bioenergy demand projections, feedstock costs are the main and most uncertain cost component for technologies without CCS while in the case with CCS payments from CO_2 removal could offset these costs (Daioglou et al., 2020). Nevertheless, costs alone cannot explain the variation in bioenergy deployment across models which is rather driven by a combination of factors like: availability of alternative mitigation options for different end-uses, availability of carbon dioxide removal and potential payments, the speed of adoption of large-scale changes in the energy conversion facilities, the relative demand for different energy services (Bauer et al., 2018; Daioglou et al., 2020). Studies investigating the barriers for the expansion to commercial scale production of perennial grasses reported that the lack of information and long-term security about the risk and return profiles of these crops are among the main impediments (Miao and Khanna, 2017; Anand et al., 2019). Costs for producing and delivering to the market biomass from perennial grasses cultivated on marginal lands in Southern Europe range between 60 and 80€ t_{DM}^{-1} (Soldatos, 2015). However, one of the main reasons for farmers investment is not the financial return, but the grass's low requirement for field operations, low maintenance cost and regeneration (Shepherd et al., 2020). Although specific numerical results of the production costs differed across literature sources and can dramatically change in time, bioenergy crop production is found to be financially feasible if conditions regarding biomass price, yield and/or government support are met (El Kasmioui and Ceulemans, 2012).

This study is assessing impacts from biomass production systems up to its delivery at farm gate excluding downstream processes like storage and conversion which will come with additional environmental impacts. Many options exist for the conversion of biomass into heat, electricity, or liquid/gaseous fuels. For example, the last IPCC report indicates conversion emission levels ranging from 1 to 31 g CO_2eq./MJ, depending on the technology and intended application (Jaramillo et al., 2022). Our site-specific estimates of environmental impacts from biomass production are suitable for being included in studies assessing different utilization pathways, so to quantify the environmental footprint of the full value chain.

4. Conclusions

The most stringent climate change mitigation pathways rely on the use of land for climate change mitigation objectives. Abandoned cropland is a promising option to increase the available area for bioenergy production at reduced risks for food security and biodiversity loss. Deployment of bioenergy is interlinked to multiple environmental dimensions, which are here assessed for three different perennial grasses and two water supply systems in Europe. Out of the total 16.2 Mha of the identified abandoned cropland in Europe between 1992 and 2015, we find that reed canary grass has the largest suitability area under rainfed conditions (88% of the identified land) and switchgrass under irrigation (with 95%).

Irrigation increases bioenergy potentials, as the land suitability increases up to 95% (15 Mha) of the total available abandoned cropland, but the impacts on climate change from the agricultural phase increase as well. However, increases in soil organic carbon are large, and in the case of production under rainfed conditions all grasses show net negative climate change impacts. For miscanthus, negative emissions are also achieved when irrigation is used. This means that cultivation of perennial grasses in Europe can store more CO_2 in the soil than the amount of GHGs released during their agricultural production and deliver negative emissions (up to 5.6% of the emissions from the agriculture sector in EU), while at the same time providing renewable energy or materials. The consideration of potential substitution of fossil-based energy and products can further increase the CO_2 mitigation benefits.

We identify relevant trade-offs among bioenergy potentials and environmental impacts. For example, switchgrass and reed canary grass can offer higher, but at generally larger environmental costs. Across all impact categories considered in this work, the southern regions of Europe show the maximum impacts under irrigated conditions. Irrigation increases bioenergy potentials, but, since it also increases the water scarcity footprint, its deployment needs to consider the local water availability and storage capacity (and many places in Southern Europe are threatened by water scarcity).

The cultivation of perennial grasses based on the energy optimization per grid cell allows to bring more area under production and to achieve the highest bioenergy potentials, which is about 7 EJ yr^{-1} (with irrigation). This corresponds to 10% of today's total primary energy consumption in Europe. Average impacts in the optimal crop mix scenarios are in between the minimum and maximum of those of the individual crops. This means that appropriate land management can deliver optimal bioenergy potential with no increased impacts. Thus, taking into consideration site-specific conditions and requirements in terms of water supply and crop affinity can help identify the best local practices to maximize energy yields and reduce environmental trade-offs in different impact categories.

CRediT authorship contribution statement

Cristina-Maria Iordan: Conceptualization, Methodology, Software, Investigation, Visualization, Writing – review & editing. **Baptiste Giroux:** Data curation, Software, Investigation, Writing – original draft. **Jan Sandstad Næss:** Investigation, Software. **Xiangping Hu:** Investigation. **Otávio Cavalett:** Conceptualization, Methodology, Validation. **Francesco Cherubini:** Conceptualization, Methodology, Writing – review & editing.

Declaration of Competing Interest

None.

Acknowledgements

The authors acknowledge the support of the Norwegian Research Council through the projects Bio4Fuels (nr. 257622), BioPath (nr. 294534), and BEST (nr. 288047). The authors are thankful to Martin Dorber and Bo Huang for helping with data acquisition. We acknowledge the *E*-OBS dataset from the EU-FP6 project UERRA (https://www.uerra.eu) and the Copernicus Climate Change Service, the data providers in the ECA&D project (https://www.ecad.eu),the GAEZ dataset (https://gaez.fao.org/) as well as the WULCA CFs (https://wulca-waterlca.org/aware/download-aware-factors/).

Appendix A. Supplementary data

Supplementary data to this article can be found online at https://doi.org/10.1016/j.eiar.2022.106942.

References

Ai, Z., Hanasaki, N., Heck, V., Hasegawa, T., Fujimori, S., 2020. Simulating second-generation herbaceous bioenergy crop yield using the global hydrological model H08 (v. bio1). Geosci. Model Dev. 13, 6077–6092.
Albanito, F., Beringer, T., Corstanje, R., Poulter, B., Stephenson, A., Zawadzka, J., Smith, P., 2016. Carbon implications of converting cropland to bioenergy crops or forest for climate mitigation: a global assessment. GCB Bioenergy 8, 81–95.
Alcamo, J., Dronin, N., Endejan, M., Golubev, G., Kirilenko, A., 2007. A new assessment of climate change impacts on food production shortfalls and water availability in Russia. Glob. Environ. Chang. 17, 429–444.
Alewell, C., Ringeval, B., Ballabio, C., Robinson, D.A., Panagos, P., Borrelli, P., 2020. Global phosphorus shortage will be aggravated by soil erosion. Nat. Commun. 11, 1–12.
Alexopoulou, E., Zanetti, F., Scordia, D., Zegada-Lizarazu, W., Christou, M., Testa, G., Cosentino, S.L., Monti, A., 2015. Long-term yields of switchgrass, giant reed, and Miscanthus in the Mediterranean basin. Bioenergy Res. 8, 1492–1499.
Alexopoulou, E., Zanetti, F., Papazoglou, E.G., Iordanoglou, K., Monti, A., 2020. Long-term productivity of thirteen lowland and upland switchgrass ecotypes in the Mediterranean region. Agronomy 10, 923.
Allen, Myles R., Fuglestvedt, Jan S., Shine, Keith P., Reisinger, Andy, Pierrehumbert, Raymond T., Forster, Piers M., 2016. New use of global warming potentials to compare cumulative and short-lived climate pollutants. Nat. Clim. Change. 6 (8), 773–776.
Amaducci, S., Facciotto, G., Bergante, S., Perego, A., Serra, P., Ferrarini, A., Chimento, C., 2017. Biomass production and energy balance of herbaceous and woody crops on marginal soils in the Po Valley. GCB Bioenergy 9, 31–45.
Anand, M., Miao, R., Khanna, M., 2019. Adopting bioenergy crops: does farmers' attitude toward loss matter? Agric. Econ. 50, 435–450.
Angelini, L.G., Ceccarini, L., Di, Nassi O., Nasso, N., Bonari, E., 2009. Comparison of Arundo donax L. and Miscanthus x giganteus in a long-term field experiment in Central Italy: Analysis of productive characteristics and energy balance. Biomass Bioenergy 33, 635–643.
Ashworth, A.J., Taylor, A.M., Reed, D.L., Allen, F.L., Keyser, P.D., Tyler, D.D., 2015. Environmental impact assessment of regional switchgrass feedstock production comparing nitrogen input scenarios and legume-intercropping systems. J. Clean. Prod. 87, 227–234.
Bai, Y., Luo, L., Van Der Voet, E., 2010. Life cycle assessment of switchgrass-derived ethanol as transport fuel. Int. J. Life Cycle Assess. 15, 468–477.
Bauer, N., Rose, S.K., Fujimori, S., Van Vuuren, D.P., Weyant, J., Wise, M., Cui, Y., Daioglou, V., Gidden, M.J., Kato, E., 2018. Global energy sector emission reductions and bioenergy use: overview of the bioenergy demand phase of the EMF-33 model comparison. Clim. Chang. 1–16.
Bond, T.C., Streets, D.G., Yarber, K.F., Nelson, S.M., Woo, J.H., Klimont, Z., 2004. A technology-based global inventory of black and organic carbon emissions from combustion. J. Geophys. Res.-Atmos. 109.
Borkowska, H., Molas, R., 2013. Yield comparison of four lignocellulosic perennial energy crop species. Biomass Bioenergy 51, 145–153.
Boulay, A.-M., Bare, J., Benini, L., Berger, M., Lathuillière, M.J., Manzardo, A., Margni, M., Motoshita, M., Núñez, M., Pastor, A.V., 2018. The Wulca consensus characterization model for water scarcity footprints: assessing impacts of water consumption based on available water remaining (AWARE). Int. J. Life Cycle Assess. 23, 368–378.
Boysen, L.R., Lucht, W., Gerten, D., 2017. Trade-offs for food production, nature conservation and climate limit the terrestrial carbon dioxide removal potential. Glob. Chang. Biol. 23, 4303–4317.
Brassard, P., Godbout, S., Pelletier, F., Raghavan, V., Palacios, J.H., 2018. Pyrolysis of switchgrass in an auger reactor for biochar production: A greenhouse gas and energy impacts assessment. Biomass Bioenergy 116, 99–105.
Bullard, M., Metcafe, P., 2001. Estimating the energy requirement and CO2 emissions from production of the prrenial grasses miscanthus switchgrass and RCG. In: Adas. Consulting Ltd (ed.).
Cai, X., Zhang, X., Wang, D., 2011. Land availability for biofuel production. Environ. Sci. Technol. 45, 334–339.
Cavalett, O., Cherubini, F., 2018. Contribution of jet fuel from forest residues to multiple Sustainable Development Goals. Nat. Sustain. 1, 799–807.
Cherubini, F., Jungmeier, G., 2010. Lca of a biorefinery concept producing bioethanol, bioenergy, and chemicals from switchgrass. Int. J. Life Cycle Assess. 15, 53–66.
Cherubini, F., Bird, N.D., Cowie, A., Jungmeier, G., Schlamadinger, B., Woess-Gallasch, S., 2009. Energy-and greenhouse gas-based LCA of biofuel and bioenergy systems: Key issues, ranges and recommendations. Resour. Conserv. Recycl. 53, 434–447.
Cherubini, F., Bright, R.M., Strømman, A.H., 2012. Site-specific global warming potentials of biogenic CO2 for bioenergy: contributions from carbon fluxes and albedo dynamics. Environ. Res. Lett. 7, 045902.
Cherubini, F., Fuglestvedt, J., Gasser, T., Reisinger, A., Cavalett, O., Huijbregts, M.A., Johansson, D.J., Jørgensen, S.V., Raugei, M., Schivley, G., 2016a. Bridging the gap between impact assessment methods and climate science. Environ. Sci. Pol. 64, 129–140.
Cherubini, F., Huijbregts, M., Kindermann, G., Van Zelm, R., Van Der Velde, M., Stadler, K., Strømman, A.H., 2016b. Global spatially explicit CO2 emission metrics for forest bioenergy. Sci. Rep. 6, 1–12.
Christian, D.G., Riche, A.B., Yates, N.E., 2008. Growth, yield and mineral content of Miscanthus×giganteus grown as a biofuel for 14 successive harvests. Ind. Crop. Prod. 28, 320–327.
Cintas, O., Berndes, G., Englund, O., Johnsson, F., 2021. Geospatial supply-demand modeling of lignocellulosic biomass for electricity and biofuels in the European Union. Biomass Bioenergy 144, 105870.
Cook-Patton, S.C., Leavitt, S.M., Gibbs, D., Harris, N.L., Lister, K., Anderson-Teixeira, K. J., Briggs, R.D., Chazdon, R.L., Crowther, T.W., Ellis, P.W., 2020. Mapping carbon accumulation potential from global natural forest regrowth. Nature 585, 545–550.
Creutzig, F., Ravindranath, N.H., Berndes, G., Bolwig, S., Bright, R., Cherubini, F., Chum, H., Corbera, E., Delucchi, M., Faaij, A., 2015. Bioenergy and climate change mitigation: an assessment. GCB Bioenergy 7, 916–944.
Daccache, A., Ciurana, J., Diaz, J.R., Knox, J.W., 2014. Water and energy footprint of irrigated agriculture in the Mediterranean region. Environ. Res. Lett. 9, 124014.
Daioglou, V., Doelman, J.C., Wicke, B., Faaij, A., Van Vuuren, D.P., 2019. Integrated assessment of biomass supply and demand in climate change mitigation scenarios. Glob. Environ. Chang. 54, 88–101.
Daioglou, V., Rose, S.K., Bauer, N., Kitous, A., Muratori, M., Sano, F., Fujimori, S., Gidden, M.J., Kato, E., Keramidas, K., 2020. Bioenergy technologies in long-run climate change mitigation: results from the EMF-33 study. Clim. Chang. 163, 1603–1620.
Davis, K.F., Rulli, M.C., Seveso, A., D'odorico, P., 2017. Increased food production and reduced water use through optimized crop distribution. Nat. Geosci. 10, 919–924.
Don, A., Osborne, B., Hastings, A., Skiba, U., Carter, M.S., Drewer, J., Flessa, H., Freibauer, A., Hyvönen, N., Jones, M.B., 2012. Land-use change to bioenergy production in E urope: implications for the greenhouse gas balance and soil carbon. GCB Bioenergy 4, 372–391.
Dubis, B., Jankowski, K.J., Załuski, D., Bórawski, P., Szempliński, W., 2019. Biomass production and energy balance of Miscanthus over a period of 11 years: a case study in a large-scale farm in Poland. GCB Bioenergy 11, 1187–1201.

Eggleston, S., Buendia, L., Miwa, K., Ngara, T., Tanabe, K., 2006. IPCC guidelines for national greenhouse gas inventories.
El Kasmioui, O., Ceulemans, R., 2012. Financial analysis of the cultivation of poplar and willow for bioenergy. Biomass Bioenergy 43, 52–64.
Elbersen, H.W., M., K., 2013. Switchgrass Ukraine. Overview of switchgrass research and guidelines. In: Research, W.U.F.B. (Ed.), Sustainable Biomass Import Program.
Elbersen, W., Poppens, R., Nbakker, R., 2013. Switchgrass (Panicum virgatum L.) A perennial biomass grass for efficient production of feedstock for the biobased economy. In: Agency, Nl, Change, N.E.A.C. (Eds.), Sustainable Biomass. Ministry of Economic Affairs, Agriculture and Innovation, Utrecht, The Netherlands.
Englund, O., Börjesson, P., Berndes, G., Scarlat, N., Dallemand, J.-F., Grizzetti, B., Dimitriou, I., Mola-Yudego, B., Fahl, F., 2020. Beneficial land use change: Strategic expansion of new biomass plantations can reduce environmental impacts from EU agriculture. Glob. Environ. Chang. 60, 101990.
Englund, O., Börjesson, P., Mola-Yudego, B., Berndes, G., Dimitriou, I., Cederberg, C., Scarlat, N., 2021. Strategic deployment of riparian buffers and windbreaks in Europe can co-deliver biomass and environmental benefits. Commun. Earth Environ. 2, 1–18.
ESA, 2017. Land Cover CCI Product User Guide Version 2. Tech. Rep.
Escobar, N., Ramírez-Sanz, C., Chueca, P., Moltó, E., Sanjuán, N., 2017. Multiyear Life Cycle Assessment of switchgrass (Panicum virgatum L.) production in the Mediterranean region of Spain: a comparative case study. Biomass Bioenergy 107, 74–85.
FAO, 2017. Irrigation in Eastern Europe in figures –AQUASTAT Survey 2016. Food and Agriculture Organization of the United Nations (FAO).
Fernando, A.L., Costa, J., Barbosa, B., Monti, A., Rettenmaier, N., 2018. Environmental impact assessment of perennial crops cultivation on marginal soils in the Mediterranean Region. Biomass Bioenergy 111, 174–186.
Field, J.L., Richard, T.L., Smithwick, E.A., Cai, H., Laser, M.S., Lebauer, D.S., Long, S.P., Paustian, K., Qin, Z., Sheehan, J.J., 2020. Robust paths to net greenhouse gas mitigation and negative emissions via advanced biofuels. Proc. Natl. Acad. Sci. 117, 21968–21977.
Finnan, J., Carroll, J., Burke, B., 2016. An evaluation of grass species as feedstocks for combustion in Ireland. In: Barth, S., Murphy-Bokern, D., Kalinina, O., Taylor, G., Jones, M. (Eds.), Perennial Biomass Crops for a Resource-Constrained.
Fischer, G., Nachtergaele, F.O., Prieler, S., Teixeira, E., Tóth, G., Van Velthuizen, H., Verelst, L., Wiberg, D., 2012. Global agro-ecological zones (GAEZ v3. 0)-model documentation.
Folberth, C., Khabarov, N., Balkovič, J., Skalský, R., Visconti, P., Ciais, P., Janssens, I.A., Peñuelas, J., Obersteiner, M., 2020. The global cropland-sparing potential of high-yield farming. Nat. Sustain. 3, 281–289.
Fonte, C., See, L., Lesiv, M., Fritz, S., 2019. A preliminary quality analysis of the climate change initiative land cover products for continental Portugal. ISPRS-Int. Arch. Photogramm. Remote Sens. Spatial Inform. Sci 42, 1213–1220.
Frischknecht, R., Jolliet, O., 2016. Global guidance for life cycle impact assessment indicators. In: Publication of the UNEP/SETAC Life Cycle Initiative, Paris, DTI/2081/PA, ISBN, pp. 978–992.
Fusi, A., Bacenetti, J., Proto, A.R., Tedesco, D.E., Pessina, D., Facchinetti, D., 2020. Pellet production from miscanthus: energy and environmental assessment. Energies 14, 73.
Georgescu, M., Lobell, D.B., Field, C.B., 2011. Direct climate effects of perennial bioenergy crops in the United States. Proc. Natl. Acad. Sci. 108, 4307–4312.
Goglio, P., Smith, W.N., Grant, B.B., Desjardins, R.L., Mcconkey, B.G., Campbell, C.A., Nemecek, T., 2015. Accounting for soil carbon changes in agricultural life cycle assessment (LCA): a review. J. Clean. Prod. 104, 23–39.
Gordon, C., Cooper, C., Senior, C.A., Banks, H., Gregory, J.M., Johns, T.C., Mitchell, J.F., Wood, R.A., 2000. The simulation of SST, sea ice extents and ocean heat transports in a version of the Hadley Centre coupled model without flux adjustments. Clim. Dyn. 16, 147–168.
Hanssen, S.V., Daioglou, V., Steinmann, Z.J., Frank, S., Popp, A., Brunelle, T., Lauri, P., Hasegawa, T., Huijbregts, M.A., Van Vuuren, D.P., 2019. Biomass residues as twenty-first century bioenergy feedstock—a comparison of eight integrated assessment models. Clim. Chang. 1–18.
Harding, K., Twine, T.E., Vanloocke, A., Bagley, J., Hill, J., 2016. Impacts of second-generation biofuel feedstock production in the central US on the hydrologic cycle and global warming mitigation potential. Geophys. Res. Lett. 43, 10,773–10,781.
Hastings, A., Clifton-Brown, J., Wattenbach, M., Mitchell, C.P., Smith, P., 2009. The development of MISCANFOR, a new Miscanthus crop growth model: towards more robust yield predictions under different climatic and soil conditions. GCB Bioenergy 1, 154–170.
Hastings, A., Mos, M., Yesufu, J.A., McCalmont, J., Schwarz, K., Shafei, R., Ashman, C., Nunn, C., Schuele, H., Cosentino, S., Scalici, G., Scordia, D., Wagner, M., Clifton-Brown, J., 2017. Economic and environmental assessment of seed and rhizome propagated miscanthus in the UK. Front. Plant Sci. 8, 1058.
Heaton, E., 2004. A quantitative review comparing the yields of two candidate C4 perennial biomass crops in relation to nitrogen, temperature and water. Biomass Bioenergy 27, 21–30.
Heikkinen, J., Keskinen, R., Kostensalo, J., Nuutinen, V., 2022. Climate change induces carbon loss of arable mineral soils in boreal conditions. Glob. Chang. Biol. 28.
Hiederer, R., Köchy, M., 2011. Global soil organic carbon estimates and the harmonized world soil database. EUR 79 (10), 2788.
Hou, W., Hou, X., 2019. Data fusion and accuracy analysis of multi-source land use/land cover datasets along coastal areas of the maritime silk road. ISPRS Int. J. Geo Inf. 8, 557.
Howard Skinner, R., Zegada-Lizarazu, W., Schmidt, J.P., 2012. Environmental impacts of switchgrass management for bioenergy production. In: Monti, A. (Ed.), Switchgrass: A Valuable Biomass Crop for Energy. Springer London, London.
Huijbregts, M.A., Steinmann, Z.J., Elshout, P.M., Stam, G., Verones, F., Vieira, M., Hollander, A., Zijp, M., Van Zelm, R., 2016. ReCiPe 2016: a harmonized life cycle impact assessment method at midpoint and endpoint level report I: characterization.
Humpenöder, F., Popp, A., Bodirsky, B.L., Weindl, I., Biewald, A., Lotze-Campen, H., Dietrich, J.P., Klein, D., Kreidenweis, U., Müller, C., 2018. Large-scale bioenergy production: how to resolve sustainability trade-offs? Environ. Res. Lett. 13, 024011.
IEA, I., 2019. World Energy Statistics and Balances. IEA, OECD, Paris (France).
IIASA/FAO, 2012. Global Agro-ecological Zones (GAEZ v3.0). Iiasa, Laxenburg, Austria and FAO, Rome, Italy.
Iordan, C.M., Verones, F., Cherubini, F., 2018. Integrating impacts on climate change and biodiversity from forest harvest in Norway. Ecol. Indic. 89, 411–421.
ISRIC, W.S.I., 2017. Global map bulk density. In: Information, W. S. (ed.).
Jaramillo, P., Kahn Ribeiro, S., Newman, P., Dhar, S., Diemuodeke, O.E., Kajino, T., Lee, D.S., Nugroho, S.B., Ou, X., Hammer Strømman, A., Whitehead, J., 2022. Transport. In: Shukla, P.R., Skea, J., Slade, R., Al Khourdajie, A., Van Diemen, R., Mccollum, D., Pathak, M., Some, S., Vyas, P., Fradera, R., Belkacemi, M., Hasija, A., Lisboa, G., Luz, S., Malley, J. (Eds.), IPCC, 2022: Climate Change 2022: Mitigation of Climate Change. *Contribution of Working Group Iii to the Sixth Assessment Report of the Intergovernmental Panel on Climate Change* Cambridge University Press, Cambridge, Uk and New York, Ny, Usa.
Jepsen, M.R., Kuemmerle, T., Müller, D., Erb, K., Verburg, P.H., Haberl, H., Vesterager, J. P., Andrič, M., Antrop, M., Austrheim, G., 2015. Transitions in European land-management regimes between 1800 and 2010. Land Use Policy 49, 53–64.
Jolliet, O., Antón, A., Boulay, A.-M., Cherubini, F., Fantke, P., Levasseur, A., Mckone, T. E., Michelsen, O., Canals, I., L. M. & Motoshita, M., 2018. Global guidance on environmental life cycle impact assessment indicators: impacts of climate change, fine particulate matter formation, water consumption and land use. Int. J. Life Cycle Assess. 23, 2189–2207.
Jones, M.B., Zimmermann, J., Clifton-Brown, J., 2016. Long-Term Yields and Soil Carbon Sequestration from Miscanthus: A Review. Springer, Cham.
Joos, F., Roth, R., Fuglestvedt, J.S., Peters, G.P., Enting, I.G., Bloh, W.V., Brovkin, V., Burke, E.J., Eby, M., Edwards, N.R., 2013. Carbon dioxide and climate impulse response functions for the computation of greenhouse gas metrics: a multi-model analysis. Atmos. Chem. Phys. 13, 2793–2825.
Karvonen, V., Ribard, C., Sädekoski, N., Tyystjärvi, V., Muukkonen, P., 2018. Comparing ESA land cover data with higher resolution national datasets. Creating, managing, and analysing geospatial data and databases in geographical themes, pp. 26–45.
Kiesel, A., Wagner, M., Lewandowski, I., 2016. Environmental performance of miscanthus, switchgrass and maize: can C4 perennials increase the sustainability of biogas production? Sustainability 9, 5.
Krzyżaniak, M., Stolarski, M.J., Warmiński, K., 2020. Life cycle assessment of giant miscanthus: production on marginal soil with various fertilisation treatments. Energies 13, 1931.
Lasanta, T., Arnáez, J., Pascual, N., Ruiz-Flaño, P., Errea, M., Lana-Renault, N., 2017. Space–time process and drivers of land abandonment in Europe. Catena 149, 810–823.
Ledo, A., Hillier, J., Smith, P., Aguilera, E., Blagodatskiy, S., Brearley, F.Q., Datta, A., Diaz-Pines, E., Don, A., Dondini, M., Dunn, J., Feliciano, D.M., Liebig, M.A., Lang, R., Llorente, M., Zinn, Y.L., Mcnamara, N., Ogle, S., Qin, Z., Rovira, P., Rowe, R., Vicente-Vicente, J.L., Whitaker, J., Yue, Q., Zerihun, A., 2019. A global, empirical, harmonised dataset of soil organic carbon changes under perennial crops. Scientific Data 6, 57.
Ledo, A., Smith, P., Zerihun, A., Whitaker, J., Vicente-Vicente, J.L., Qin, Z., Mcnamara, N.P., Zinn, Y.L., Llorente, M., Liebig, M., Kuhnert, M., Dondini, M., Don, A., Diaz-Pines, E., Datta, A., Bakka, H., Aguilera, E., Hillier, J., 2020. Changes in soil organic carbon under perennial crops. Glob. Chang. Biol. 26, 4158–4168.
Leirpoll, M.E., Næss, J.S., Cavalett, O., Dorber, M., Hu, X., Cherubini, F., 2021. Optimal combination of bioenergy and solar photovoltaic for renewable energy production on abandoned cropland. Renew. Energy 168, 45–56.
Levers, C., Schneider, M., Prishchepov, A.V., Estel, S., Kuemmerle, T., 2018. Spatial variation in determinants of agricultural land abandonment in Europe. Sci. Total Environ. 644, 95–111.
Lewandowski, I., 2016. The Role of Perennial Biomass Crops in a Growing Bioeconomy. Springer, Cham.
Lewandowski, I., Scurlock, J.M.O., Lindvall, E., Christou, M., 2003. The development and current status of perennial rhizomatous grasses as energy crops in the US and Europe. Biomass Bioenergy 25, 335–361.
Li, S., Li, X., 2017. Global understanding of farmland abandonment: a review and prospects. J. Geogr. Sci. 27, 1123–1150.
Li, W., Ciais, P., Makowski, D., Peng, S., 2018. A global yield dataset for major lignocellulosic bioenergy crops based on field measurements. Scientific data 5, 1–10.
Li, W., Ciais, P., Stehfest, E., Van Vuuren, D., Popp, A., Arneth, A., Di Fulvio, F., Doelman, J., Humpenöder, F., Harper, A.B., 2020. Mapping the yields of lignocellulosic bioenergy crops from observations at the global scale. Earth Syst. Sci. Data 12, 789–804.
Li, J., Xiong, F., Chen, Z., 2021. An integrated life cycle and water footprint assessment of nonfood crops based bioenergy production. Sci. Rep. 11, 3912.
Liang, L., Liu, Q., Liu, G., Li, H., Huang, C., 2019. Accuracy evaluation and consistency analysis of four global land cover products in the Arctic Region. Remote Sens. 11, 1396.
Liu, W., Yan, J., Li, J., Sang, T., 2012. Yield potential of miscanthus energy crops in the Loess Plateau of China. GCB Bioenergy 4, 545–554.
Liu, L., Xu, X., Hu, Y., Liu, Z., Qiao, Z., 2018. Efficiency analysis of bioenergy potential on winter fallow fields: A case study of rape. Sci. Total Environ. 628, 103–109.

Liu, H., Gong, P., Wang, J., Clinton, N., Bai, Y., Liang, S., 2020. Annual dynamics of global land cover and its long-term changes from 1982 to 2015. Earth Syst. Sci.Data 12, 1217–1243.
Lowe, J., 2005. IPCC DDC AR4 UKMO-HadCM3 SRESA1B run1. World Data Center for Climate (WDCC) at DKRZ. http://cera-www.dkrz.de/Wdcc/ui/Compact.jsp?acronym=Ukmo_HadCM3_SRESA1B_1.
Maggi, F., Tang, F.H., La Cecilia, D., Mcbratney, A., 2019. PEST-CHEMGRIDS, global gridded maps of the top 20 crop-specific pesticide application rates from 2015 to 2025. Scientific data 6, 1–20.
Majumdar, K., Norton, R.M., Murrell, T.S., García, F., Zingore, S., Prochnow, L.I., Pampolino, M., Boulal, H., Dutta, S., Francisco, E., 2021. Assessing potassium mass balances in different countries and scales. In: Improving potassium recommendations for agricultural crops, p. 283.
McCalmont, J.P., Hastings, A., Mcnamara, N.P., Richter, G.M., Robson, P., Donnison, I.S., Clifton-Brown, J., 2017. Environmental costs and benefits of growing Miscanthus for bioenergy in the UK. GCB Bioenergy 9, 489–507.
McElwee, P., Calvin, K., Campbell, D., Cherubini, F., Grassi, G., Korotkov, V., Le Hoang, A., Lwasa, S., Nkem, J., Nkonya, E., 2020. The impact of interventions in the global land and agri-food sectors on Nature's Contributions to People and the UN Sustainable Development Goals. Glob. Chang. Biol. 26, 4691–4721.
Miao, R., Khanna, M., 2017. Effectiveness of the biomass crop assistance program: roles of behavioral factors, credit constraint, and program design. Appl. Econ. Perspect. Policy 39, 584–608.
Miller, J.N., Vanloocke, A., Gomez-Casanovas, N., Bernacchi, C.J., 2016. Candidate perennial bioenergy grasses have a higher albedo than annual row crops. GCB Bioenergy 8, 818–825.
Muri, H., 2018. The role of large—scale BECCS in the pursuit of the 1.5 C target: an Earth system model perspective. Environ. Res. Lett. 13, 044010.
Murphy, F., Devlin, G., Mcdonnell, K., 2013. Miscanthus production and processing in Ireland: An analysis of energy requirements and environmental impacts. Renew. Sust. Energ. Rev. 23, 412–420.
Myhre, G., Shindell, D., Bréon, F., Collins, W., Fuglestvedt, J., Huang, J., Koch, D., Lamarque, J., Lee, D., Mendoza, B., 2013. Climate change 2013: the physical science basis. Contribution of working group I to the fifth assessment report of the intergovernmental panel on climate change, pp. 659–740.
Næss, J.S., Cavalett, O., Cherubini, F., 2021. The land–energy–water nexus of global bioenergy potentials from abandoned cropland. Nat. Sustain. 4, 525–536.
Næss, J.S., Iordan, C.M., Muri, H., Cherubini, F., 2022. Energy potentials and water requirements from perennial grasses on abandoned land in the former Soviet Union. Environ. Res. Lett. 17, 045017.
Nemecek, T., Kägi, T., Blaser, S., 2007. Life cycle inventories of agricultural production systems. Final report ecoinvent v2. 0 No, 15.
Oliveira, J.A., West, C., Afif, E., Palencia, P., 2017. Comparison of miscanthus and switchgrass cultivars for biomass yield, soil nutrients, and nutrient removal in northwest Spain. Agron. J. 109, 122–130.
Pahkala, K., Aalto, M., Isolahti, M., Poikola, J., Jauhiainen, L., 2008. Large-scale energy grass farming for power plants—a case study from Ostrobothnia, Finland. Biomass Bioenergy 32, 1009–1015.
Pereira, L.G., Cavalett, O., Bonomi, A., Zhang, Y., Warner, E., Chum, H.L., 2019. Comparison of biofuel life-cycle Ghg emissions assessment tools: the case studies of ethanol produced from sugarcane, corn, and wheat. Renew. Sust. Energ. Rev. 110, 1–12.
Perić, M., Komatina, M., Antonijević, D., Bugarski, B., DŽeletović, Ž., 2018. Life cycle impact assessment of miscanthus crop for sustainable household heating in Serbia. Forests 9, 1–26.
Petersen, B.M., Knudsen, M.T., Hermansen, J.E., Halberg, N., 2013. An approach to include soil carbon changes in life cycle assessments. J. Clean. Prod. 52, 217–224.
Popp, A., Calvin, K., Fujimori, S., Havlik, P., Humpenöder, F., Stehfest, E., Bodirsky, B.L., Dietrich, J.P., Doelmann, J.C., Gusti, M., 2017. Land-use futures in the shared socio-economic pathways. Glob. Environ. Chang. 42, 331–345.
Potter, P., Ramankutty, N., Bennett, E.M., Donner, S.D., 2010. Characterizing the spatial patterns of global fertilizer application and manure production. Earth Interact. 14, 1–22.
Powlson, D.S., Riche, A., Shield, I., 2005. Biofuels and other approaches for decreasing fossil fuel emissions from agriculture. Ann. Appl. Biol. 146, 193–201.
Qin, Zhangcai, Dunn, Jennifer B., Kwon, Hoyoung, Mueller, Steffen, Wander, Michelle M., 2016. Soil carbon sequestration and land use change associated with biofuel production: empirical evidence. Gcb Bioenergy 1 (8), 66–80.
Rahman, S.A., Baral, H., Sharma, R., Samsudin, Y.B., Meyer, M., Lo, M., Artati, Y., Simamora, T.I., Andini, S., Leksono, B., 2019. Integrating bioenergy and food production on degraded landscapes in Indonesia for improved socioeconomic and environmental outcomes. Food Energy Security 8, e00165.
Ramesh, T., Bolan, N.S., Kirkham, M.B., Wijesekara, H., Kanchikerimath, M., Rao, C.S., Sandeep, S., Rinklebe, J., Ok, Y.S., Choudhury, B.U., 2019. Soil organic carbon dynamics: Impact of land use changes and management practices: a review. Adv. Agron. 156, 1–107.
Robertson, A.D., Whitaker, J., Morrison, R., Davies, C.A., Smith, P., Mcnamara, N.P., 2017a. A Miscanthus plantation can be carbon neutral without increasing soil carbon stocks. GCB Bioenergy 9, 645–661.
Robertson, G.P., Hamilton, S.K., Barham, B.L., Dale, B.E., Izaurralde, R.C., Jackson, R.D., Landis, D.A., Swinton, S.M., Thelen, K.D., Tiedje, J.M., 2017b. Cellulosic biofuel contributions to a sustainable energy future: choices and outcomes. Science 356.
Rogelj, J., Shindell, D., Jiang, K., Fifita, S., Forster, P., Ginzburg, V., Handa, C., Kheshgi, H., Kobayashi, S., Kriegler, E., 2018. Mitigation pathways compatible with 1.5 C in the context of sustainable development.
Rosenzweig, C., Elliott, J., Deryng, D., Ruane, A.C., Müller, C., Arneth, A., Boote, K.J., Folberth, C., Glotter, M., Khabarov, N., 2014. Assessing agricultural risks of climate change in the 21st century in a global gridded crop model intercomparison. Proc. Natl. Acad. Sci. 111, 3268–3273.
Samson, R., Delaquis, E., Deen, B., Debruyn, J., Eggiman, U., 2016. Switchgrass agronomy. In: Ontario Biomass Producers Co-Operative Inc (ed.).
Sanscartier, D., Deen, B., Dias, G., Maclean, H.L., Dadfar, H., Mcdonald, I., Kludze, H., 2014. Implications of land class and environmental factors on life cycle GHG emissions of Miscanthus as a bioenergy feedstock. GCB Bioenergy 6, 401–413.
Santoro, M., Kirches, G., Wevers, J., Boettcher, M., Brockmann, C., Lamarche, C., Defourny, P., 2017. Land Cover CCI: Product User Guide Version 2.0. Climate Change Initiative Belgium.
Schmidt, T., Fernando, A., Monti, A., Rettenmaier, N., 2015. Life cycle assessment of bioenergy and bio-based products from perennial grasses cultivated on marginal land in the Mediterranean Region. BioEnergy Res 8, 1548–1561.
Scordia, D., Cosentino, S., 2019. Perennial energy grasses: resilient crops in a changing European agriculture. Agriculture 9, 169.
Serra, P., Giuntoli, J., Agostini, A., Colauzzi, M., Amaducci, S., 2017. Coupling sorghum biomass and wheat straw to minimise the environmental impact of bioenergy production. J. Clean. Prod. 154, 242–254.
Shepherd, A., Clifton-Brown, J., Kam, J., Buckby, S., Hastings, A., 2020. Commercial experience with miscanthus crops: establishment, yields and environmental observations. GCB Bioenergy 12, 510–523.
Shukla, P., Skea, J., Calvo Buendia, E., Masson-Delmotte, V., Pörtner, H., Roberts, D., Zhai, P., Slade, R., Connors, S., Van Diemen, R., 2019. IPCC, 2019: Climate Change and Land: an IPCC special report on climate change, desertification, land degradation, sustainable land management, food security, and greenhouse gas fluxes in terrestrial ecosystems.
Shurpali, N.J., Strandman, H., Kilpeläinen, A., Huttunen, J., Hyvönen, N., Biasi, C., Kellomäki, S., Martikainen, P.J., 2010. Atmospheric impact of bioenergy based on perennial crop (reed canary grass, Phalaris arundinaceae, L.) cultivation on a drained boreal organic soil. GCB Bioenergy 2, 130–138.
Slade, R., Bauen, A., Gross, R., 2014. Global bioenergy resources. Nat. Clim. Chang. 4, 99–105.
Smeets, E.M.W., Lewandowski, I.M., Faaij, A.P.C., 2009. The economical and environmental performance of miscanthus and switchgrass production and supply chains in a European setting. Renew. Sust. Energ. Rev. 13, 1230–1245.
Smith, P., Haberl, H., Popp, A., Erb, K.H., Lauk, C., Harper, R., Tubiello, F.N., De Siqueira Pinto, A., Jafari, M., Sohi, S., 2013. How much land-based greenhouse gas mitigation can be achieved without compromising food security and environmental goals? Glob. Chang. Biol. 19, 2285–2302.
Smith, P., Adams, J., Beerling, D.J., Beringer, T., Calvin, K.V., Fuss, S., Keesstra, S., 2019. Impacts of land-based greenhouse gas removal options on ecosystem services and the United Nations sustainable development goals. Annu. Rev. Environ. Resour. 44, 255–286.
Smith, P., Calvin, K., Nkem, J., Campbell, D., Cherubini, F., Grassi, G., Korotkov, V., Le Hoang, A., Lwasa, S., Mcelwee, P., 2020. Which practices co-deliver food security, climate change mitigation and adaptation, and combat land degradation and desertification? Glob. Chang. Biol. 26, 1532–1575.
Soldatos, P., 2015. Economic aspects of bioenergy production from perennial grasses in marginal lands of South Europe. BioEnergy Res 8, 1562–1573.
Staples, M., Olcay, H., Malina, R., Trivedi, P., Pearlson, M., Strzepek, K., Paltsev, S., Wollersheim, C., Barrett, S., 2013. Water consumption footprint and land requirements of large-scale alternative diesel and jet fuel production. Environ. Sci. Technol. 47, 12557–12565.
Staples, M.D., Malina, R., Barrett, S.R.H., 2017. The limits of bioenergy for mitigating global life-cycle greenhouse gas emissions from fossil fuels. Nat. Energy 2, 16202.
Tadele, D., Roy, P., Defersha, F., Misra, M., Mohanty, A.K., 2019. Life Cycle Assessment of renewable filler material (biochar) produced from perennial grass (Miscanthus). Aims Energy 7, 430.
Tanaka, K., Cavalett, O., Collins, W.J., Cherubini, F., 2019. Asserting the climate benefits of the coal-to-gas shift across temporal and spatial scales. Nat. Clim. Chang. 9, 389–396.
TNO, E, 2020. Phyllis2-Database for (Treated) Biomass, Algae, Feedstocks for Biogas Production and Biochar. Von Phyllis2, Database for (treated) Biomass, Algae, Feedstocks for Biogas …..
Tsendbazar, N.-E., De Bruin, S., Mora, B., Schouten, L., Herold, M., 2016. Comparative assessment of thematic accuracy of GLC maps for specific applications using existing reference data. Int. J. Appl. Earth Obs. Geoinf. 44, 124–135.
Ustaoglu, E., Collier, M.J., 2018. Farmland abandonment in Europe: an overview of drivers, consequences, and assessment of the sustainability implications. Environ. Rev. 26, 396–416.
Van Duren, I., Voinov, A., Arodudu, O., Firrisa, M.T., 2015. Where to produce rapeseed biodiesel and why? Mapping European rapeseed energy efficiency. Renew. Energy 74, 49–59.
Wagner, M., Kiesel, A., Hastings, A., Iqbal, Y., Lewandowski, I., 2017. Novel Miscanthus germplasm-based value chains: a life cycle assessment. Front. Plant Sci. 8, 990.
Wernet, G., Bauer, C., Steubing, B., Reinhard, J., Moreno-Ruiz, E., Weidema, B., 2016. The ecoinvent database version 3 (part I): overview and methodology. Int. J. Life Cycle Assess. 21, 1218–1230.
Xu, X., Wang, L., Cai, H., Wang, L., Liu, L., Wang, H., 2017. The influences of spatiotemporal change of cultivated land on food crop production potential in China. Food Security 9, 485–495.
Zhu, X., Liang, C., Masters, M.D., Kantola, I.B., Delucia, E.H., 2018. The impacts of four potential bioenergy crops on soil carbon dynamics as shown by biomarker analyses and DRIFT spectroscopy. GCB Bioenergy 10, 489–500.